Biphasic Regulation of Yes-associated Protein (YAP) Cellular Localization, Phosphorylation, and Activity by G Protein-coupled Receptor Agonists in Intestinal Epithelial Cells

A NOVEL ROLE FOR PROTEIN KINASE D (PKD)*

Jia Wang[‡], James Sinnett-Smith[‡§¶], Jan V. Stevens[‡], Steven H. Young[‡¶], and Enrique Rozengurt[‡§¶‖1]

From the [‡]Division of Digestive Diseases, Department of Medicine, David Geffen School of Medicine, [§]CURE: Digestive Diseases Research Center, and [‖]Molecular Biology Institute, UCLA, Los Angeles, California 90095 and the [¶]Veterans Affairs Greater Los Angeles Health Care System, Los Angeles, California 90073

We examined the regulation of Yes-associated protein (YAP) localization, phosphorylation, and transcriptional activity in intestinal epithelial cells. Our results show that stimulation of intestinal epithelial IEC-18 cells with the G protein-coupled receptor (GPCR) agonist angiotensin II, a potent mitogen for these cells, induced rapid translocation of YAP from the nucleus to the cytoplasm (within 15 min) and a concomitant increase in YAP phosphorylation at Ser^{127} and Ser^{397}. Angiotensin II elicited YAP phosphorylation and cytoplasmic accumulation in a dose-dependent manner (ED_{50} = 0.3 nM). Similar YAP responses were provoked by stimulation with vasopressin or serum. Treatment of the cells with the protein kinase D (PKD) family inhibitors CRT0066101 and kb NB 142-70 prevented the increase in YAP phosphorylation on Ser^{127} and Ser^{397} via Lats2, YAP cytoplasmic accumulation, and increase in the mRNA levels of YAP/TEAD-regulated genes (*Ctgf* and *Areg*). Furthermore, siRNA-mediated knockdown of PKD1, PKD2, and PKD3 markedly attenuated YAP nuclear-cytoplasmic shuttling, phosphorylation at Ser^{127}, and induction of *Ctgf* and *Areg* expression in response to GPCR activation. These results identify a novel role for the PKD family in the control of biphasic localization, phosphorylation, and transcriptional activity of YAP in intestinal epithelial cells. In turn, YAP and TAZ are necessary for the stimulation of the proliferative response of intestinal epithelial cells to GPCR agonists that act via PKD. The discovery of interaction between YAP and PKD pathways identifies a novel crosstalk in signal transduction and demonstrates, for the first time, that the PKDs feed into the YAP pathway.

The proliferation of the epithelial cells of the intestinal mucosa is a tightly regulated process modulated by a broad range of regulatory peptides, neurotransmitters, bioactive lipids, and differentiation signals (1). Many of these stimuli initiate their characteristic effects in their target cells through G protein-coupled receptors (GPCRs)[2] (2–6). Despite their fundamental importance for understanding intestinal homeostasis, wound healing, and pathogenesis of human diseases, the intracellular signal transduction mechanisms that mediate GPCR-induced proliferation of intestinal epithelial cells remain incompletely understood.

The highly conserved Hippo pathway, originally identified in *Drosophila*, is attracting intense interest as a key regulator of organ size, tissue regeneration, tumorigenesis, and GPCR signaling (7). Canonical Hippo signals in vertebrate cells are transduced through a core serine/threonine kinase cascade wherein Mst1/2 kinases, in complex with the scaffold Sav1, phosphorylate and activate Lats1/2 (large tumor suppressor 1//2), in complex with its regulatory protein MOB1/2 (8). In addition to Mst1/2, Hppy/MAP4Ks were recently identified as alternative kinases that phosphorylate Lats1/2 (9, 10). In turn, Lats1/2 phosphorylates the transcriptional co-activators Yes-associated protein (YAP) and WW-domain-containing transcriptional co-activator with PDZ-binding motif (TAZ), two major downstream effectors of the Hippo pathway. The intracellular distribution of YAP and TAZ is highly dynamic, exhibiting rapid nuclear-cytoplasmic shuttling. The phosphorylation of YAP and TAZ by Lats1/2 is widely thought to restrict their activity, cellular localization, and stability. In the absence of phosphorylation, YAP localizes to the nucleus where it binds and activates the TEA domain DNA-binding transcription factors thereby stimulating the expression of proliferative and anti-apoptotic genes. Several studies indicate that YAP acts as a context-specific oncogene (11) and that the Hippo pathway inhibits its activity. Despite intense interest in this novel pathway, many important questions relating to its function remain unanswered as follows: 1) the mechanism(s) by which upstream signals feed into the Hippo cascade remain incompletely defined; 2) YAP not only acts as a transcriptional co-activator in the nucleus but also mediates biological functions in other cellular locations, including the cytoplasm (12, 13); and 3) YAP crosstalks with other important signaling pathways, but the biologi-

[1] To whom correspondence should be addressed: 900 Veteran Ave., Warren Hall Rm. 11-124, Dept. of Medicine, UCLA School of Medicine, Los Angeles, CA 90095-1786. Tel.: 310-794-6610; E-mail: erozengurt@mednet.ucla.edu.

[2] The abbreviations used are: GPCR, G protein-coupled receptor; YAP, Yes-associated protein; ANG II, angiotensin II; qPCR, quantitative PCR; LMB, leptomycin B; NES, nuclear export sequence; AT₁, ANG II type 1; TRITC, tetramethylrhodamine isothiocyanate.

cal outcome (positive or negative) of these interactions remains unclear and is likely cell context-dependent. Even at the most fundamental level, the precise role of YAP in intestinal epithelial cell proliferation remains incompletely understood, as evidence for both growth-stimulatory and growth-suppressive roles of YAP/TAZ has been presented (14–17).

GPCR agonists act as important signals upstream of the Hippo/YAP/TAZ pathway. Protein kinase D (PKD), a protein kinase family within the Ca^{2+}/calmodulin-dependent kinase group (18), has emerged as a prominent downstream signal induced by GPCRs that function through $G\alpha_{q/11}$, $G\alpha_{12}$, $G\alpha_i$, and Rho (18–26). PKD1, the founding and most studied member of the PKD family (27, 28), which is composed of PKD1, PKD2, and PKD3, is rapidly activated through protein kinase C (PKC)-mediated phosphorylation of Ser^{744} and Ser^{748} in the PKD1 activation loop (29–32). PKD1 catalytic activation within cells leads to its auto-phosphorylation at Ser^{916} and Ser^{748} (33–36). Rapid PKC-dependent PKD1 activation is followed by a late PKC-independent phase of activation induced by GPCR agonists (35–37). Accumulating evidence demonstrates that the PKD family plays an important role in a variety of cellular processes and activities, including cytoskeletal organization, gene expression, cell migration, and proliferation (19). In intestinal epithelial cells, PKD1 activation mediates migration and proliferation both *in vitro* and *in vivo* (36, 38). Accordingly, multiple growth-promoting stimuli rapidly activate PKD1 catalytic activity in intestinal epithelial cells (23, 36, 38–40) through activation loop phosphorylation (30, 35–37). Furthermore, transgenic mice that express elevated PKD1 protein in intestinal epithelial cells display a marked increase in DNA-synthesizing cells in their intestinal crypts and a significant increase in the length and total number of cells per crypt (36). Collectively, these results support the notion that PKD1 signaling is a novel element in the pathway leading to proliferation of intestinal epithelial cells *in vitro* and *in vivo*. The mechanisms downstream of PKD1, however, remain to be elucidated, and in particular, cross-talk between PKD and YAP has not been identified either in intestinal epithelial cells or in any other cell type.

The results presented here identify a novel temporal pattern of nuclear-cytoplasmic shuttling of endogenous YAP in response to GPCR stimulation in intestinal epithelial cells. Specifically, we show that GPCR activation elicits a rapid but transient YAP phosphorylation and localization to the cytoplasm followed by a second phase involving YAP re-localization to the nucleus and stimulation of YAP/TEAD-regulated genes. Further studies demonstrate, for the first time, cross-talk between PKD and Lats/YAP/TEAD signaling pathways. Based on the results presented here, we conclude that the PKD family controls the localization, phosphorylation, and transcriptional co-activator activity of YAP in intestinal epithelial cells. In turn, YAP is necessary for the stimulation of the proliferative response of intestinal epithelial cells to GPCR agonists that act via PKD. Collectively, our results identify, for the first time, a novel cross-talk between YAP and PKD signaling pathways leading to biphasic regulation of YAP in intestinal epithelial cells.

Results

Identification of a Novel Pattern of YAP Nuclear-Cytoplasmic Shuttling in Intestinal Epithelial Cells—To examine the regulation of YAP cellular localization, phosphorylation, and activity in intestinal epithelial cells, we used the non-transformed IEC-18 and IEC-6 cells (41, 42), which were derived from neonatal rat small intestine and have characteristics of crypt-type epithelial cells. These cells endogenously express $G\alpha_{q/11}$-coupled receptors for angiotensin II (ANG II) and vasopressin (23, 39, 40, 43–46) and have been extensively used as a model system to examine signal transduction pathways in response to GPCR activation (23, 36, 38, 39, 43–45, 47). ANG II and vasopressin act as potent growth factors for IEC-18 and IEC-6 cells (23, 39, 43–45, 47). Because the levels of YAP/TAZ influence their association with transcriptional cofactors especially when expressed at elevated levels, we studied the localization, phosphorylation, and activity of the endogenous YAP protein.

Initially, we determined the localization of YAP in confluent and quiescent cultures of IEC-18 cells (23, 36) after various times of stimulation with or without ANG II. In unstimulated cells, YAP was localized to the nucleus and cytoplasm, as revealed by immunofluorescence staining using antibodies that detect total YAP. In contrast to results presented in other cells types, stimulation of IEC-18 cells with ANG II induced a rapid and dramatic translocation of YAP from the nucleus to the cytoplasm (Fig. 1*A*). Using the CellProfiler software for image analysis, we quantified the nuclear to cytoplasmic ratio of YAP immunofluorescence in thousands of individual cells. This analysis revealed that nuclear YAP declined steeply (within 15 min) and transiently in response to ANG II stimulation (Fig. 1*B*). YAP re-localized to the nucleus after 2 h of stimulation. The histogram representing the distribution of control cells as a function of their nuclear to cytoplasmic ratio of YAP followed a normal distribution (Fig. 1*C*, *open bars*). Treatment of IEC-18 cells with ANG II for 30 min caused a marked shift of the distribution to the left (Fig. 1*C*, *closed bars*), reflecting YAP translocation from the nucleus to the cytoplasm in most cells of the population. Rapid nuclear-cytoplasmic shuttling of YAP was also provoked by stimulation of IEC-18 cells with the GPCR agonist vasopressin (39) or by serum growth factors (Fig. 1*D*).

In dose-response studies, ANG II induced rapid cytoplasmic localization of YAP in IEC-18 cells even at concentrations lower than 1 nM (Fig. 2*A*). Quantification by image analysis indicates that half-maximal effect of ANG II was elicited at 0.3 nM (Fig. 2*B*), suggesting that this agonist regulates YAP localization in intestinal epithelial cells via its specific endogenous GPCRs. Indeed, pretreatment of IEC-18 cells with the selective ANG II type 1 (AT_1) receptor antagonist losartan completely blocked ANG II-induced YAP nuclear extrusion (Fig. 2*C*). Surprisingly, our results revealed that mitogenic stimuli, including GPCR agonists and serum growth factors, induce biphasic re-distribution of YAP in intestinal epithelial IEC-18 cells characterized by rapid cytoplasmic localization followed by subsequent nuclear re-localization, a temporal pattern distinct from that induced by mitogenic stimuli in other cell types.
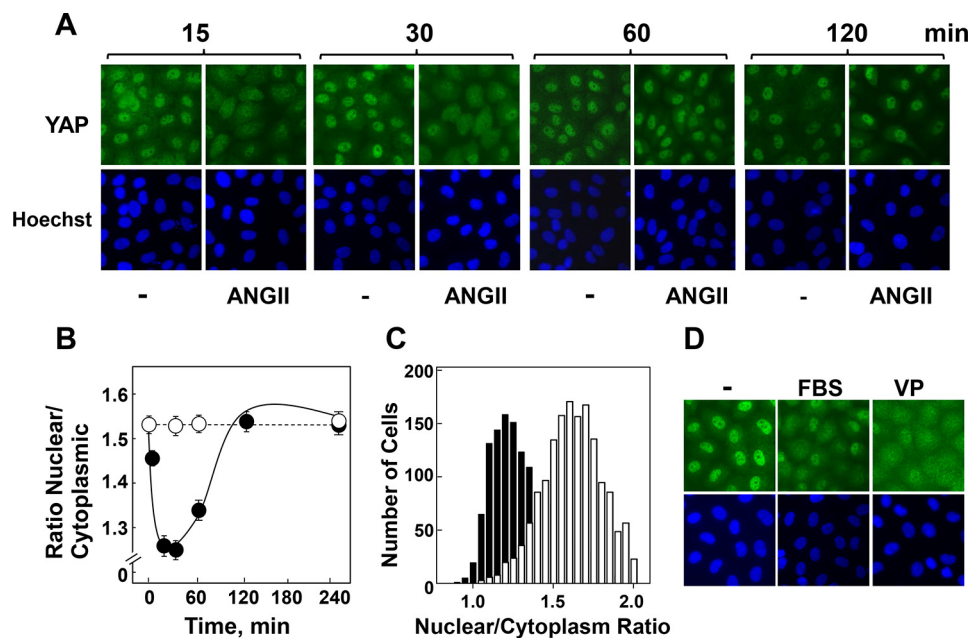
FIGURE 1. **ANG II induces rapid YAP cytoplasmic localization in intestinal epithelial IEC-18 cells.** *A,* confluent and quiescent cultures of IEC-18 cells were stimulated without (−) or with 10 nM ANG II for the indicated times. The cultures were then washed, fixed with 4% paraformaldehyde, and stained with an antibody that detects total YAP and with Hoechst 33342 to visualize the cell nuclei. *B,* quantification of the images shown in *A* was determined with the CellProfiler software, as described under "Experimental Procedures." The plot shown represents the mean nuclear/cytoplasmic ratios of YAP immunofluorescence ± S.E. $n = 8$ fields (~1400 cells were analyzed for each time point). Similar results were obtained in three independent experiments. *C, histogram* represents the distribution of control and ANG II-stimulated cells (at 30 min) as a function of their nuclear/cytoplasmic ratio of YAP immunofluorescence based on the analysis of ~1700 cells from one experiment. Similar results were obtained in 10 independent experiments. *D,* confluent cultures of IEC-18 cells were stimulated without (−) or with either 10% FBS (*FBS*) or 50 nM vasopressin (*VP*) for 30 min. The cultures were then washed, fixed with 4% paraformaldehyde, and stained with an antibody that detects total YAP and with Hoechst 33342 to visualize the cell nuclei. Similar results were obtained in three independent experiments.

GPCR Agonists Induce Rapid Increase in the Phosphorylation of YAP at Ser^{127} and Ser^{397} in IEC-18 Cells—We next determined whether ANG II-induced activation of endogenous AT_1 receptors modulates YAP phosphorylation at Ser^{127}, a highly conserved residue located within a consensus sequence phosphorylated by Lats1/2 (H*X*R*XX*S). Cultures of IEC-18 cells were stimulated with ANG II for various times, and cell lysates were analyzed by Western blotting with an antibody that detects the phosphorylated state of YAP at Ser^{127}. ANG II induced a rapid and transient increase in YAP phosphorylation at Ser^{127} in intestinal epithelial cells (Fig. 3*A*). An increase in YAP phosphorylation was detected within 5 min of stimulation and reached a maximum within 15 min. The time course of the increase in YAP phosphorylation coincided with the rapid cytoplasmic localization of YAP (shown in Fig. 1).

To examine further whether YAP localization and phosphorylation of Ser^{127} are tightly coupled in IEC-18 cells, cultures of these cells were challenged with increasing concentrations of ANG II for 30 min, and cell lysates were analyzed by Western blotting to detect the phosphorylated state of YAP at Ser^{127}. As shown in Fig. 3*B*, ANG II elicited YAP phosphorylation at Ser^{127} in a dose-dependent manner. Half-maximal stimulation was achieved at ~0.3 nM, implying that the dose responses of ANG II for eliciting rapid increase in YAP phosphorylation at Ser^{127} (Fig. 3*C*) and cytoplasmic localization (shown in Fig. 2*B*) are virtually superimposable.

In addition to Lats1/2, mammalian NDR1/2 kinases have recently been proposed to phosphorylate YAP on Ser^{127} in the intestinal epithelial cells (48). Interestingly, the NDRs (<u>n</u>uclear <u>dbf2-r</u>elated) did not phosphorylate YAP at Ser^{397} (48), a residue targeted by Lats1/2 (49). Consequently, we determined whether GPCR stimulation induces YAP phosphorylation at Ser^{397}. Treatment with ANG II induced a rapid (Fig. 3*A*) and dose-dependent (Fig. 3*B*) increase in YAP phosphorylation at Ser^{397}. Indeed, the dose responses of ANG II for eliciting YAP phosphorylation at Ser^{127} and Ser^{397} were identical (Fig. 3*C*).

We verified that the bands detected with the phospho-specific Ser^{127} (Ser(P)^{127}) and Ser^{397} (Ser(P)^{397}) antibodies correspond to endogenous YAP because Western blotting analysis of YAP immunoprecipitates with the Ser(P)^{127} or Ser(P)^{397} antibodies revealed a single band that co-migrated with YAP (Fig. 3*D*). In addition, the bands detected with the Ser(P)^{127} and Ser(P)^{397} antibodies were completely extinguished by siRNA-mediated knockdown of YAP (Fig. 3*E*). The results imply that stimulation of IEC-18 cells with ANG II induces rapid and transient increase in YAP phosphorylation at Ser^{127} and Ser^{397} that coincided with the rapid re-distribution of this transcriptional co-activator from the nucleus to the cytoplasm.

GPCR Agonists Induce Rapid Increase in the Phosphorylation of YAP in IEC-6 and Caco-2 Intestinal Epithelial Cells—Rapid cytoplasmic localization and phosphorylation of YAP in response to GPCR agonists was not restricted to IEC-18 cells but detected in other intestinal cells, including IEC-6 cells stimulated with ANG II (Fig. 4*A*) and in human epithelial colorectal adenocarcinoma Caco-2 cells challenged with serum (Fig. 4*B*). These findings are of great interest as they indicate that rapid translocation of YAP from the nucleus to cytoplasm and phos-
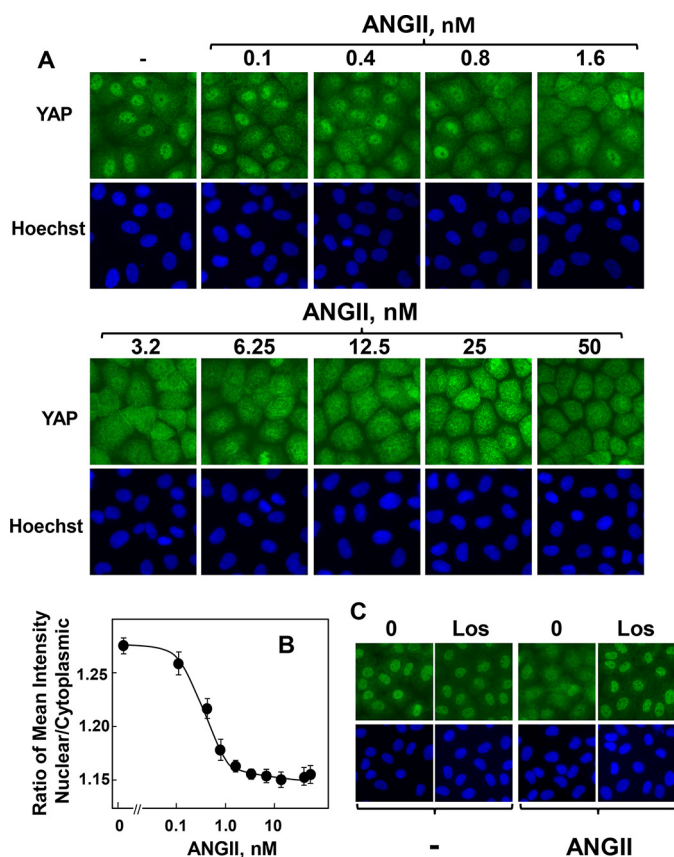
FIGURE 2. ANG II induces YAP cytoplasmic localization in a dose-dependent manner via the AT₁ receptor in IEC-18 cells. *A,* confluent cultures of IEC-18 cells were stimulated with ANG II at the indicated concentrations for 30 min. The cultures were then washed, fixed with 4% paraformaldehyde, and stained with an antibody that detects total YAP and with Hoechst 33342 to visualize the cell nuclei. *B,* quantification of nuclear/cytoplasmic ratio of YAP immunofluorescence shown in *A* was determined with the CellProfiler software as described under "Experimental Procedures." The plot shown are the mean ratios ± S.E. *n* = 7 fields (∼1250 cells were analyzed for each concentration of ANG II). Similar results were obtained in a separate experiment. *C,* confluent cultures of IEC-18 cells were incubated without (*0*) or with the selective ANG II type 1 (*AT₁*) receptor antagonist losartan (*Los*) at 10 μM for 30 min prior to stimulation with 10 nM ANG II for 30 min. The cultures were then washed, fixed with 4% paraformaldehyde, and stained with an antibody that detects total YAP and with Hoechst 33342 to visualize the cell nuclei. Similar results were obtained in three independent experiments.

phorylation occurs in a variety of intestinal epithelial cells stimulated to proliferate by multiple stimuli.

Because our results with mitogen-stimulated intestinal epithelial cells contrasted sharply with previous reports typically using HEK293 cells, we also examined YAP localization and phosphorylation in these cells, using our reagents and experimental conditions. We readily confirmed that YAP was in the cytoplasm of densely plated HEK293 cells and that serum (or lysophosphatidic acid) stimulation of these cells promoted rapid YAP nuclear import and dephosphorylation at Ser^{127} (Fig. 4*C*). Indeed, the decrease in YAP phosphorylation at Ser^{127} induced by serum or lysophosphatidic acid was striking after 30 min of stimulation and persisted for at least 4 h (Fig. 4*C*). Similarly, stimulation of human pancreatic cancer PANC-1 cells with neurotensin, a neuropeptide that acts through endogenously expressed GPCRs in these cells (50, 51), promoted rapid YAP nuclear import and dephosphorylation at Ser^{127} (Fig. 4*D*). The results substantiate that growth-promoting GPCR ago-

nists and serum growth factors induce a distinct pattern of YAP intracellular redistribution and phosphorylation in intestinal epithelial cells, clearly different from the sequence of these events observed in either HEK293 or PANC-1 cells.

Role of Akt, PKA, and PKC in Mediating Intracellular Translocation and Phosphorylation of YAP in Intestinal Epithelial Cells—As a first step to identify upstream pathways that mediate rapid GPCR-induced YAP nuclear-cytoplasmic shuttling in intestinal epithelial cells, we tested small molecule inhibitors targeting kinases. Given the purported role of Akt in Hippo pathway regulation in other cell types (52, 53), we initially determined the effect of the Akt inhibitor GSK690693 (54) on YAP re-localization and phosphorylation. Treatment of intact IEC-18 cells with 2.5 μM GSK690693 blocked the rapid cytoplasmic accumulation of YAP induced by stimulation with ANG II (Fig. 5*A*). Image analysis revealed that exposure to GSK690693 completely prevented the decrease in the nuclear to cytoplasmic ratio of YAP induced by ANG II (Fig. 5*B*). Similar results were obtained when IEC-18 cells were stimulated with vasopressin or serum instead of ANG II (data not shown). Furthermore, GSK690693 inhibited YAP phosphorylation at both Ser^{127} and Ser^{397} in intestinal epithelial IEC-18 cells (Fig. 5*C*).

To confirm the specificity of the effects obtained with GSK690693, we tested other Akt inhibitors, including GDC-0068, a structurally unrelated ATP-competitive inhibitor of the Akt family (55), and MK2206, an allosteric inhibitor that binds to the pleckstrin homology domain of the Akts (56). Surprisingly, neither GDC-0068 at 2.5 μM nor MK2206 at 5 μM had any effect on the cytoplasmic translocation of YAP induced by ANG II in IEC-18 cells (Fig. 5, *A* and *B*). Furthermore, these compounds did not prevent YAP phosphorylation at Ser^{127} or Ser^{397} (Fig. 5*C*). We verified that exposure of IEC-18 cells to either 2.5 μM GDC-0068 or 5 μM MK2206 inhibited Akt activation as effectively as GSK690693, as scored by the phosphorylation of PRAS40 phosphorylation at Thr^{246}, a residue targeted by Akt (Fig. 5*C*). These results implied that GSK690693 potently inhibits YAP cytoplasmic localization and phosphorylation in IEC-18 cells through an Akt-independent pathway.

In addition to Akt, GSK690693 also inhibits PKA and novel PKCs (57). Therefore, we tested whether inhibition of these kinases has any effect on YAP localization and/or phosphorylation in IEC-18 cells. Exposure to H89 at 10 μM, a concentration that suppresses PKA activity within intact IEC-18 cells,[3] did not produce any detectable effect on either YAP localization (Fig. 5, *D,* image analysis in *E*) or phosphorylation (Fig. 5*F*) in response to ANG II. In sharp contrast, treatment with the PKC inhibitors Gö6983 or GF1 prior to ANG II stimulation greatly attenuated YAP cytoplasmic localization (Fig. 5, *D,* image analysis in *E*) and phosphorylation at both Ser^{127} and Ser^{397} (Fig. 5*F*). These results implied that PKCs mediate transient YAP re-localization and phosphorylation in GPCR-stimulated IEC-18 cells.

PKDs Mediate Intracellular Translocations and Phosphorylation of YAP—We previously demonstrated that the PKCs phosphorylate PKD at the T-loop leading to its catalytic activation

---

[3] J. Wang, J. Sinnett-Smith, and E. Rozengurt, unpublished results.
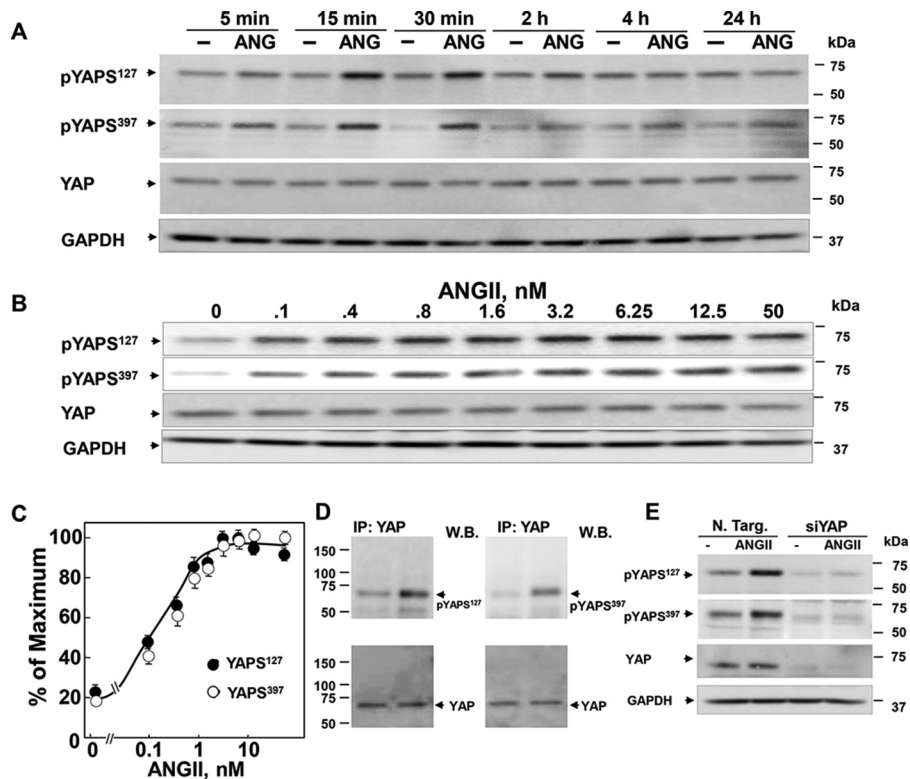
FIGURE 3. **ANG II induces rapid increase in the phosphorylation of YAP at Ser[127] and Ser[397] in IEC-18 cells.** *A* and *B,* confluent cultures of IEC-18 cells were incubated without (−) or with ANG II (*ANG*) for the indicated times (*A*) or concentrations (*B*). Cultures were then lysed with 2× SDS-PAGE sample buffer and analyzed by immunoblotting with antibodies that detect YAP phosphorylated at Ser[127] and Ser[397]. Immunoblotting for total YAP and GADPH was also included. *C,* quantification of total YAP phosphorylated at Ser[127] and Ser[397] was performed using MultiGauge version 3.0. The results represent the mean ± S.E., $n = 3$, and are expressed as percentage of the maximal level of YAP phosphorylated at Ser[127] and Ser[397]. Similar results were obtained in three independent experiments. *D,* confluent cultures of IEC-18 cells were stimulated with 10 nm ANG II for 30 min. Then the cells were lysed, and YAP immunoprecipitates (*IP: YAP*) were analyzed by Western blotting (*W.B.*) with YAP Ser[127] and Ser[397]. *E,* cultures of IEC-18 cells were transfected with non-targeting siRNA (*N. Targ*) or with siRNAs targeting YAP for 4 days. The cultures were then stimulated with 10 nm ANG II for 30 min. Cells were lysed with 2× SDS-PAGE sample buffer and analyzed by immunoblotting antibodies that detect YAP phosphorylated at Ser[127] and Ser[397], total YAP, and GAPDH. Similar results were obtained in four independent experiments.
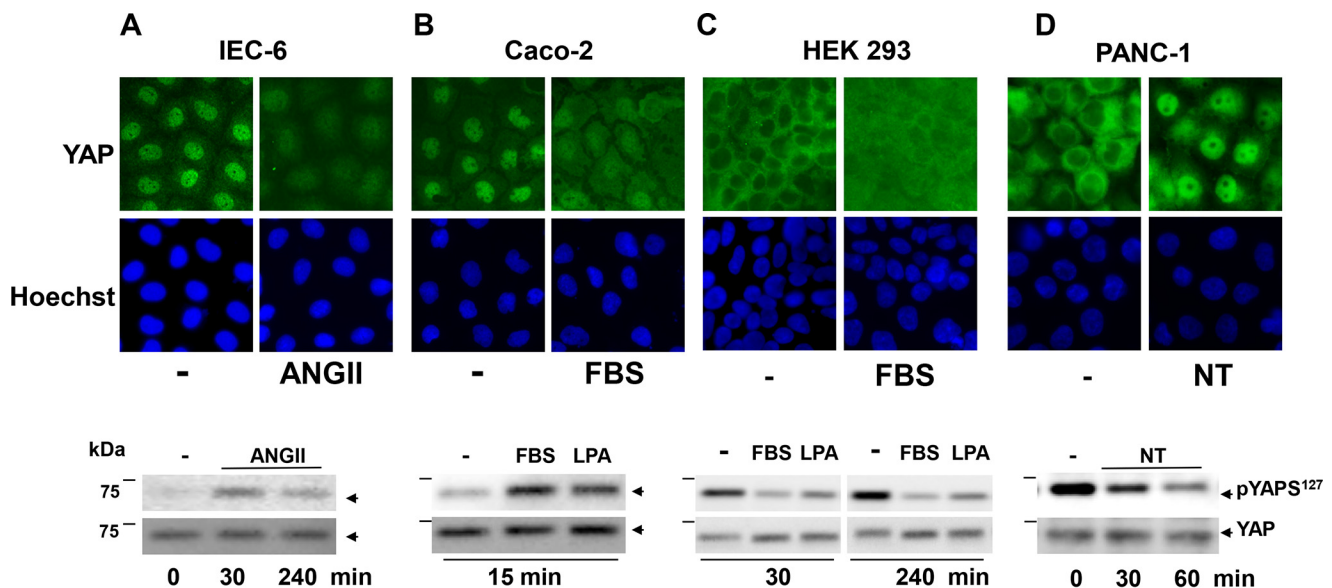

FIGURE 4. **GPCR agonists and serum induce cytoplasmic localization and phosphorylation of YAP in IEC-6 and Caco-2 intestinal epithelial cells.** *A–D, upper,* confluent cultures of IEC-6 (*A*), Caco-2 (*B*), HEK293 (*C*), and PANC-1 (*D*) cells were stimulated with 10 nm ANG II (*A*), 10% FBS (*B* and *C*), or 10 nm neurotensin (*NT*) (*D*), as indicated. The cultures were then washed, fixed with 4% paraformaldehyde, and stained with an antibody that detects total YAP and with Hoechst 33342 to visualize the cell nuclei. *A–D, lower,* confluent cultures of IEC-6 (*A*), Caco-2 (*B*), HEK293 (*C*), and PANC-1 (*D*) cells were stimulated with 10 nm ANG II (*A*), 10% FBS or 10 μm lysophosphatidic acid (*LPA*) (*B* and *C*), or 10 nm neurotensin (*NT*) (*D*) for the indicated times. Cultures were then lysed with 2× SDS-PAGE sample buffer and analyzed by immunoblotting antibodies that detect YAP phosphorylated at Ser[127] and total YAP. Similar results were obtained in at least two independent experiments.
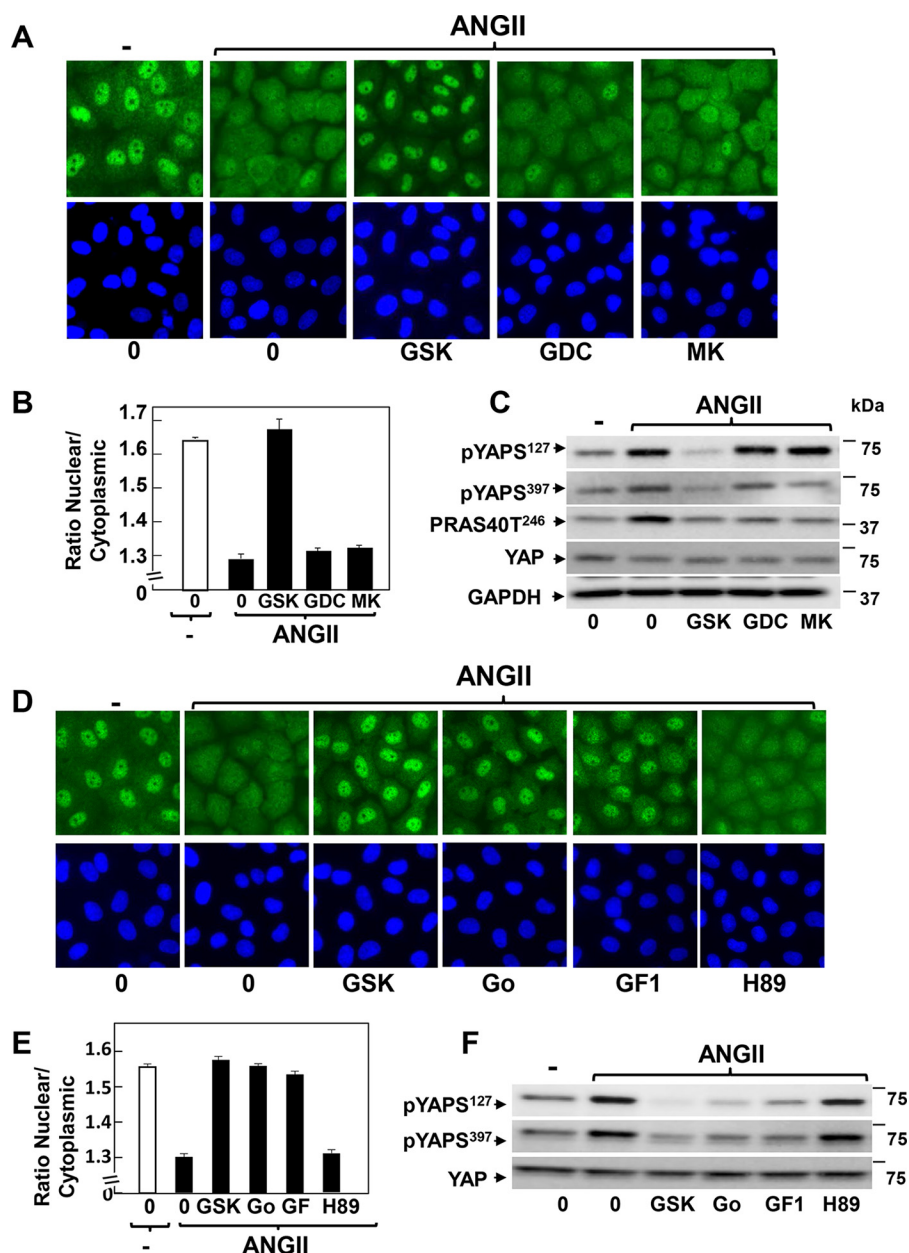
FIGURE 5. **ANG II induces cytoplasmic localization and phosphorylation of YAP through an Akt-independent but PKC-dependent pathway in IEC-18 cells.** *A,* confluent cultures of IEC-18 cells were incubated in the absence (*0*) or presence of 2.5 μM GSK690693 (*GSK*), 2.5 μM GDC-0068 (*GDC*), or 5 μM MK2206 (*MK*) for 1 h prior to stimulation of the cells without (−) or with 10 nM ANG II for 30 min. The cultures were then washed, fixed with 4% paraformaldehyde, and stained with an antibody that detects total YAP and with Hoechst 33342 to visualize the cell nuclei. *B,* quantification of the nuclear/cytoplasmic ratio of YAP immunofluorescence shown in *A* was determined with the CellProfiler software. The *bars* shown are the mean nuclear/cytoplasmic ratio ± S.E. *n* = 6 fields (~1,200 cells were analyzed for each condition). Similar results were obtained in three independent experiments. *C,* confluent cultures of IEC-18 cells were incubated in the absence (*0*) or presence of 2.5 μM GSK690693 (*GSK*), 2.5 μM GDC-0068 (*GDC*), or 5 μM MK2206 (*MK*) for 1 h prior to stimulation of the cells without (−) or with 10 nM ANG II for 30 min. Cells were then lysed with 2× SDS-PAGE sample buffer and analyzed by immunoblotting with antibodies that detect YAP phosphorylated at either Ser[127] or Ser[397], PRAS40 phosphorylated at Thr[246], and total YAP and GADPH. Similar results were obtained in three independent experiments. *D,* confluent cultures of IEC-18 cells were incubated in the absence (*0*) or presence of 2.5 μM GSK690693 (*GSK*), 5 μM Gö6983 (*Go*), 5 μM GF1, or 10 μM H89 for 1 h prior to stimulation of the cells without (−) or with 10 nM ANG II for 30 min. The cultures were then washed, fixed with 4% paraformaldehyde, and stained with an antibody that detects total YAP and with Hoechst 33342 to visualize the cell nuclei. *E,* quantification of the nuclear/cytoplasmic ratio of YAP immunofluorescence shown in *D* was determined with the CellProfiler software. The *bars* shown are the mean nuclear/cytoplasmic ratios ± S.E. *n* = 6 fields (~1,100 cells were analyzed for each condition). Similar results were obtained in four independent experiments. *F,* confluent cultures of IEC-18 cells were incubated in the absence (*0*) or presence of 2.5 μM GSK690693 (*GSK*), 5 μM Gö6983 (*Go*), 5 μM GF1, or 10 μM H89 for 1 h prior to stimulation of the cells without (−) or with 10 nM ANG II for 30 min. Cells were then lysed with 2× SDS-PAGE sample buffer and analyzed by immunoblotting antibodies that detect YAP phosphorylated at Ser[127] and Ser[397] and total YAP. Similar results were obtained in three independent experiments.

(31, 32). Accordingly, treatment with either Gö6983 or GSK690693 greatly attenuated PKD1 auto-phosphorylation at Ser[916] induced by either ANG II or serum (data not shown). Treatment with GSK690693 also inhibited PKD phosphoryla-tion at Ser[744], a residue in the activation loop phosphorylated by PKCs (data not shown). Consequently, we next examined whether the PKDs mediate the effects of mitogenic GPCR ago-nists on YAP localization and phosphorylation. To test this pos-
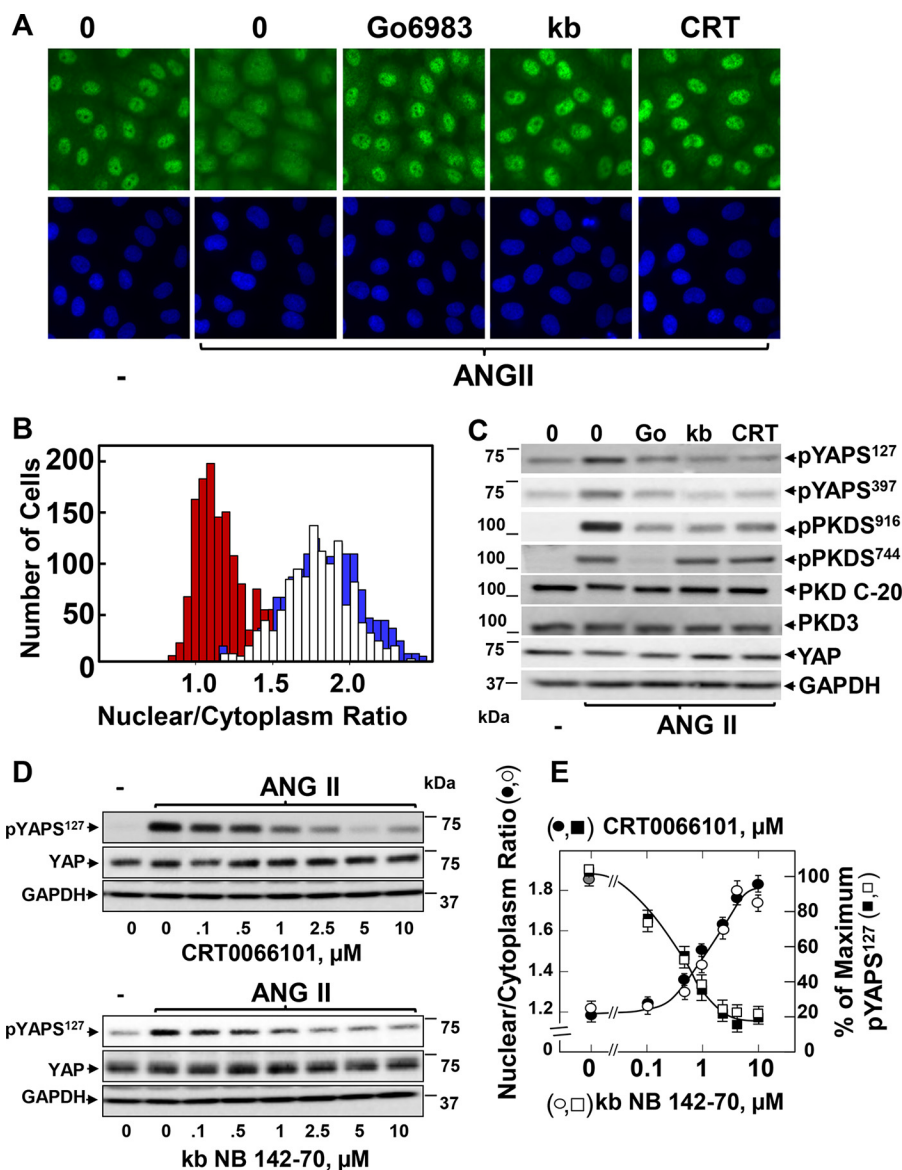
FIGURE 6. **PKD family inhibitors prevent transient YAP translocation and phosphorylation in response to ANG II in IEC-18 cells.** *A,* confluent cultures of IEC-18 cells were incubated in the absence (*0*) or presence of 5 μM Gö6983, 3.5 μM kb NB 142-70 (*kb*), or 2.5 μM CRT0066101 (*CRT*) for 1 h prior to stimulation of the cells without (−) or with 10 nM ANG II for 30 min. The cultures were then washed, fixed with 4% paraformaldehyde, and stained with an antibody that detects total YAP and with Hoechst 33342 to visualize the cell nuclei. *B,* quantification of the nuclear/cytoplasmic ratio of YAP immunofluorescence was determined using CellProfiler. The *bars* shown represent control (*open bars*), ANG II (*red bars*), ANG II + CRT (*blue bars*) and are the nuclear/cytoplasmic ratios from ~1,000 cells from one experiment. Similar results were obtained in six independent experiments. *C,* confluent cultures of IEC-18 cells were incubated in the absence (*0*) or presence of 5 μM Gö6983 (*Go*), 3.5 μM kb NB 142-70 (*kb*), or 2.5 μM CRT0066101 (*CRT*) for 1 h prior to stimulation of the cells without (−) or with 10 nM ANG II for 30 min. Cells were then lysed with 2× SDS-PAGE sample buffer and analyzed by immunoblotting antibodies that detect YAP phosphorylated at Ser[127] and Ser[397], PKD1 phosphorylated at Ser[916], PKDs phosphorylated at Ser[744], and total PKD1/2 (PKD C-20), PKD3, YAP, and GAPDH. Similar results were obtained in six independent experiments. *D* and *E,* confluent cultures of IEC-18 cells were incubated in the absence (*0*) or presence of increasing concentrations of either CRT0066101 (*closed squares,* in *E*) or kb NB 142-70 (*open squares* in *E*) for 1 h prior to stimulation of the cells without (−) or with 10 nM ANG II for 30 min. Cells were then lysed with 2× SDS-PAGE sample buffer and analyzed by immunoblotting antibodies that detect YAP phosphorylated at Ser[127], total YAP, and GAPDH. Quantification YAP Ser[127] phosphorylation (shown in *E*) was performed using MultiGauge version 3.0. The results represent the mean ± S.E., *n* = 3, and are expressed as percentage of the maximum level of YAP Ser[127]. *E,* confluent cultures of IEC-18 cells incubated in the absence (*gray circle*) or presence of increasing concentrations of CRT0066101 (*closed circles*) or kb NB 142-70 (*open circles*) for 1 h as indicated prior to stimulation of the cells without or with 10 nM ANG II for 30 min. The cultures were then washed, fixed with 4% paraformaldehyde, and stained with an antibody that detects total YAP and with Hoechst 33342 to visualize the cell nuclei and analyzed with the CellProfiler software. The results shown are the nuclear/cytoplasmic ratio of YAP immunofluorescence ± S.E.; ~700 cells were analyzed at each concentration of CRT0066101 (*closed circles*) or kb NB 142-70 (*open circles*). Similar results were obtained in two independent experiments.

sibility, we used two structurally unrelated selective inhibitors of PKD activity, CRT0066101 (58) and kb NB 142-70. In previous studies, we demonstrated that these inhibitors block PKD activation and DNA synthesis in IEC-18 cells (36, 38, 59, 60). As shown in Fig. 6*A*, exposure of IEC-18 cells to CRT0066101 or kb NB 142-70 prevented YAP redistribution in response to ANG II

as effectively as Gö6983. Image analysis verified that the marked YAP translocation from the nucleus to the cytoplasm induced by ANG II was greatly diminished by cell treatment with CRT0066101 (Fig. 6*B*, *histogram*). Remarkably, CRT0066101 and kb NB 142-70 inhibited YAP phosphorylation at both Ser[127] and Ser[397] (Fig. 6*C*). In dose-response stud-
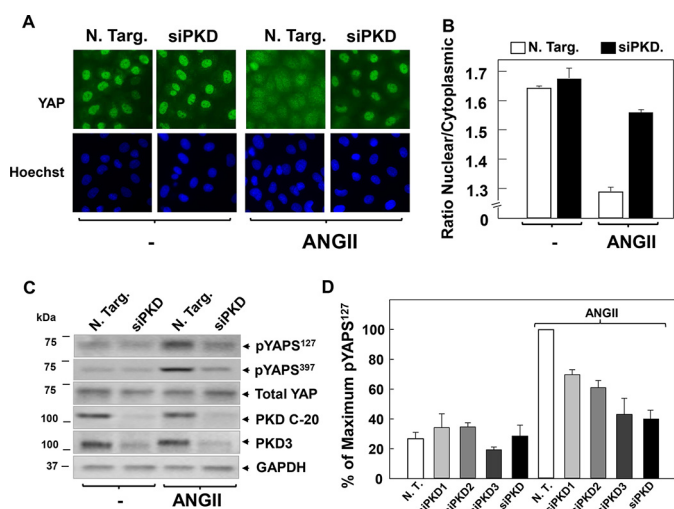
FIGURE 7. **Knockdown of PKD family expression prevents YAP transloca-tion and phosphorylation in response to ANG II in IEC-18 cells.** *A*, cultures of IEC-18 cells were transfected with non-targeting siRNA (*N. Targ*) or with a mixture of siRNAs targeting PKD1, PKD2, and PKD3 (*siPKD*) for 4 days. Then the cultures were stimulated with 10 nM ANG II for 30 min, washed, fixed with 4% paraformaldehyde, and stained with an antibody that detects total YAP and with Hoechst 33342 to visualize the cell nuclei. *B*, quantification of the nucle-ar/cytoplasmic ratio of YAP immunofluorescence shown in *A* was determined with the CellProfiler software. The *bars* shown are the mean nuclear/cytoplas-mic ratio ± S.E., $n = 10$ fields (~1,800 cells were analyzed for each condition). Similar results were obtained in four independent experiments. *C*, cultures of IEC-18 cells were transfected with non-targeting siRNA (*N. Targ*) or with a mixture of siRNAs targeting PKD1, PKD2, and PKD3 (*siPKD*) for 4 days. Then the cultures were stimulated with 10 nM ANG II for 30 min, lysed with 2× SDS-PAGE sample buffer, and analyzed by immunoblotting with antibodies that detect YAP phosphorylated at Ser[127] or Ser[397] and total YAP, PKD1/2 (PKD C-20), PKD3, and GAPDH. Similar results were obtained in four independent experiments. *D*, cultures of IEC-18 cells were transfected with non-targeting siRNA (*N. T.*) or with siRNAs targeting individual PKD1, PKD2, or PKD3 and with a mixture of siRNAs targeting the three isoforms (*siPKD*) for 4 days. Then the cultures were stimulated with 10 nM ANG II for 30 min. Cells were then lysed with 2× SDS-PAGE sample buffer and analyzed by immunoblotting with antibod-ies that detect YAP phosphorylated at Ser[127]. Quantification of YAP phosphor-ylated at Ser[127] was performed using MultiGauge version 3.0. The results rep-resent the mean ± S.E., $n = 4$, and are expressed as percentage of the maximal level of YAP phosphorylated at Ser[127]. Similar results were obtained in four independent experiments.

ies, CRT0066101 and kb NB 142-70 prevented the increase in YAP phosphorylation on Ser[127] and YAP cytoplasmic accumu-lation at similar concentrations (Fig. 6, *D*, quantification in *E*).

The effects of PKD inhibition on YAP localization and phos-phorylation were not restricted to ANG II or IEC-18 cells. Treatment with CRT0066101 inhibited rapid cytoplasmic localization and phosphorylation of YAP in response to vaso-pressin or serum in IEC-18 cells (data not shown). We also verified that CRT0066101 prevented YAP re-distribution in response to ANG II or vasopressin in IEC-6 cells (data not shown). These results suggested that PKD signaling is required for GPCR-induced YAP localization and phosphorylation in intestinal epithelial cells.

To corroborate that the PKD family plays a key role in the regulation of YAP translocation and phosphorylation, we used small interfering RNA (siRNA)-mediated knockdown of PKD1, PKD2, and PKD3 (Fig. 7). Transfection of a mixture of siRNAs targeting the three PKDs markedly attenuated YAP cytoplas-mic localization (Fig. 7, *A*, image analysis in *B*) and phosphory-lation at Ser[127] (Fig. 7C) in response to GPCR activation. We also determined the effect produced by siRNA-mediated

knockdown of the individual PKD isoforms on YAP phosphor-ylation at Ser[127]. As shown in Fig. 7D, knockdown of each PKD isoform attenuated the phosphorylation of YAP at Ser[127], with a more pronounced inhibitory effect elicited by knockdown of PKD3. These results demonstrated, for the first time, that the PKDs feed into the YAP pathway, as shown by YAP nuclear-cytoplasmic shuttling and phosphorylation in intestinal epithe-lial cells.

Stimulation of GPCR/PKD Induces YAP Localization and Phosphorylation via Lats2—As mentioned previously, GPCR/ PKD stimulation induced YAP phosphorylation at highly con-served residues (Ser[127] and Ser[397]) located within a consensus sequence phosphorylated by the Hippo core kinases Lats1/2. We therefore determined whether Lats1/2 is activated in response to ANG II via PKD in IEC-18 cells. As shown in Fig. 8A, ANG II induced a rapid increase in Lats1/2 activity (detect-able within 2.5 min), as scored by its phosphorylation at Thr[1079] (Thr[1041] in Lats2), residues located in the hydrophobic C-ter-minal domain targeted by Mst1/2 and critical for Lats1/2 acti-vation (8). In the same lysates, we verified that ANG II induced an even faster activation of PKD (prominent within 1 min) sug-gesting that PKDs act upstream of Lats in GPCR-stimulated IEC-18 cells. In line with this possibility, the increase in Lats phosphorylation at either Thr[1079] or Ser[909] (a residue located within the activation loop of the kinase catalytic domain) induced by ANG II was blunted by treatment with the PKD inhibitors CRT0066101 or kb NB 142-70 (Fig. 8B). Further-more, knockdown of Lats2 (but not Lats1) prevented the increase in YAP phosphorylation at Ser[127] and Ser[397] as well as extinguished the signals corresponding to Lats phosphoryla-tion at the T-loop and hydrophobic C-terminal domain (Fig. 8C). Furthermore, siRNA-mediated knockdown of Lats2 pre-vented the rapid nuclear extrusion of YAP induced by stimula-tion with ANG II (Fig. 8, *D*, image analysis in *E*). These results imply that stimulation of GPCR/PKD induces rapid Lats2 acti-vation leading to YAP phosphorylation and transient cytoplas-mic localization in IEC-18 cells. These rapid responses are clearly different from a feedback loop involving transcriptional regulation of YAP/TAZ and Lats2 described in other cell types (61).

GPCR Activation Induces Expression of Areg and Ctgf through PKD in Intestinal Epithelial Cells—The results presented thus far indicate that PKDs play a critical role in mediating the first phase of YAP re-distribution and phosphorylation via Lats2. The changes in YAP localization and phosphorylation were transient, as YAP phosphorylation declined and translocated to the nucleus. We hypothesized that during this second phase of YAP re-localization to the nucleus, YAP couples to TEAD tran-scription factors and promotes YAP/TEAD transcription. To examine the impact of GPCR signaling on the expression of YAP/TEAD-regulated genes in intestinal epithelial cells, we determined the expression of *Ctgf* (connective tissue growth factor) and *Areg* (amphiregulin), which are well established YAP/TEAD-regulated genes (7). We found that stimulation of IEC-18 cells with ANG II for 1 h increased the mRNA levels of *Ctgf* (3.6 ± 1.4-fold; $n = 20$) and *Areg* (14 ± 1.4-fold; $n = 16$) assayed by RT-qPCR. Knockdown of YAP/TAZ with siRNAs averted the increase in the expression of these genes (Fig. 9, *A*
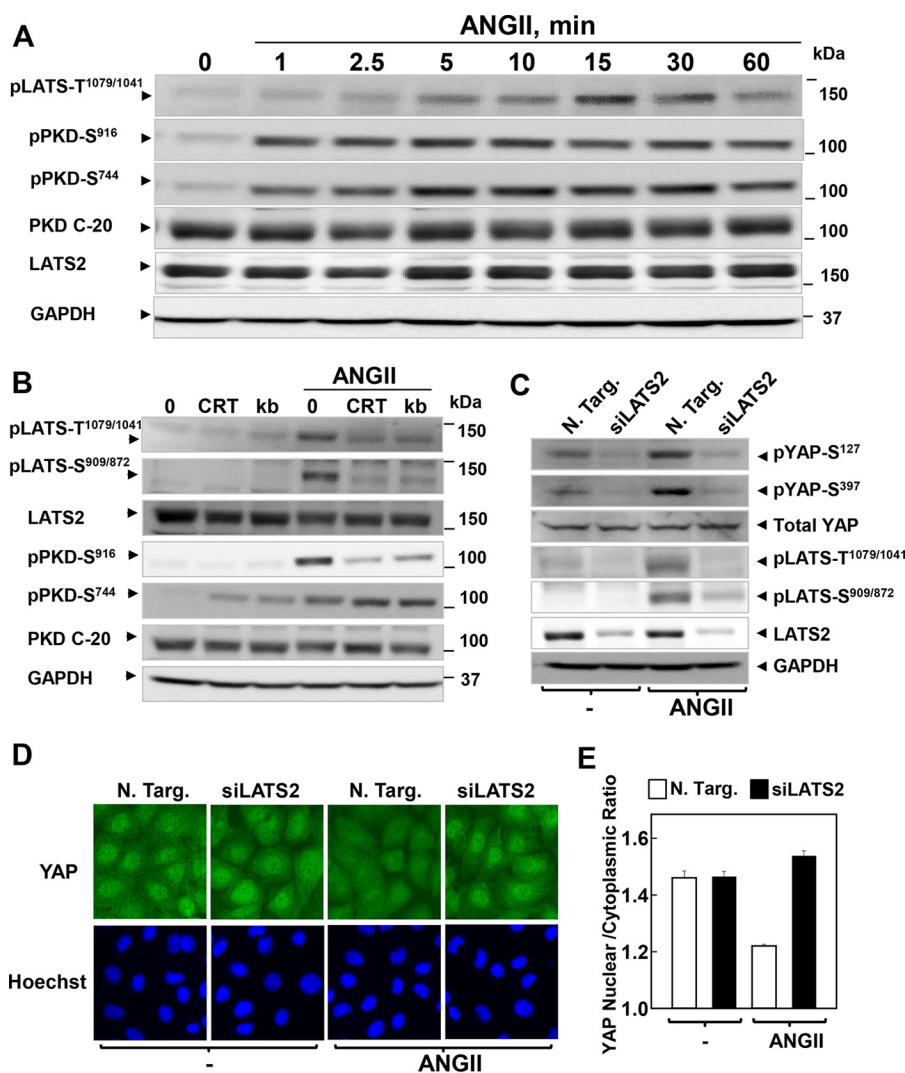
FIGURE 8. **GPCR/PKD induces a transient activation of Lats leading to YAP localization and phosphorylation in IEC-18 cells.** *A,* confluent cultures of IEC-18 cells were incubated without (*0*) or with 10 nM ANG II for the indicated times. Cultures were then lysed with 2× SDS-PAGE sample buffer and analyzed by immunoblotting antibodies that detect Lats1/2 phosphorylated at Thr$^{1079/1041}$, PKD1 phosphorylated at Ser^{916}, PKDs phosphorylated at Ser^{744}, total PKD1/2 (*PKD C-20*), total Lats2, and GAPDH. Similar results were obtained in two independent experiments. *B,* confluent cultures of IEC-18 cells were incubated in the absence (*0*) or presence of 2.5 μM CRT0066101 (*CRT*) or 3.5 μM kb NB 142-7 (*kb*) for 1 h prior to stimulation of the cells without or with 10 nM ANG II for 30 min. Cells were then lysed with 2× SDS-PAGE sample buffer and analyzed by immunoblotting antibodies that detect Lats1/2 phosphorylated at Thr$^{1079/1041}$ and Ser$^{909/872}$, PKD1 phosphorylated at Ser^{916}, PKDs phosphorylated at Ser^{744}, total PKD1/2 (PKD C-20), total Lats2, and GAPDH. Similar results were obtained in two independent experiments. *C,* cultures of IEC-18 cells were transfected with non-targeting siRNA (*N. Targ.*) or with siRNAs targeting Lats2 for 4 days. Then the cultures were stimulated with 10 nM ANG II for 30 min, lysed with 2× SDS-PAGE sample buffer, and analyzed by immunoblotting with antibodies that detect YAP phosphorylated at Ser^{127} and Ser^{397}, total YAP, Lats1/2 phosphorylated at Thr$^{1079/1041}$ and Ser$^{909/872}$, total Lats2, and GAPDH. Note that siRNA-mediated knockdown of Lats2 extinguished the signals detected with the phospho-Lats1/2 antibodies, implying that Lats2 is the predominant Lats kinase expressed endogenously by IEC-18 cells. Similar results were obtained in three independent experiments. *D,* cultures of IEC-18 cells were transfected with non-targeting siRNA (*N. Targ*) or with siRNAs targeting Lats2 for 4 days. The cultures were stimulated with 10 nM ANG II for 30 min. Then cultures were washed, fixed with 4% paraformaldehyde, and stained with an antibody that detects total YAP and with Hoechst 33342 to visualize the cell nuclei. *E,* quantification of the nuclear/cytoplasmic ratio of YAP immunofluorescence shown in *D* was determined with the CellProfiler software. The *bars* shown are the mean nuclear/cytoplasmic ratio ± S.E. *n* = 5 fields (~900 cells). Similar results were obtained in three independent experiments.

and *D*), confirming that ANG II induces *Ctgf* and *Areg* expression through YAP/TAZ during the second phase of GPCR-mediated YAP/TAZ regulation.

We next determined whether PKDs are implicated in mediating the second phase of GPCR-induced YAP activation. Exposure of intact IEC-18 cells to the PKD family inhibitors CRT0066101 or kb NB 142-70 prevented the increase of *Ctgf* and *Areg* mRNA levels in response to ANG II. (Fig. 9, *B* and *E*). These results suggested that GPCR signaling stimulates YAP/TEAD transcriptional activity in intestinal epithelial cells through PKDs. In agreement with this conclusion, transfection

of siRNAs targeting the three PKDs abrogated the increase of *Ctgf* and *Areg* mRNA levels in response to GPCR activation (Fig. 9, *C* and *F*). We also determined the inhibitory effect produced by siRNA-mediated knockdown of the individual PKD isoforms on the expression of *Ctgf* and *Areg* mRNA levels in response to GPCR activation. Knockdown of each isoform attenuated the increase in *Ctgf* mRNA, with complete suppression produced by knockdown of all PKDs (Fig. 9*G*). Similar results were obtained when the *Areg* mRNA levels were determined (data not shown). Collectively, our findings identify a novel function for PKDs in mediating GPCR-induced YAP
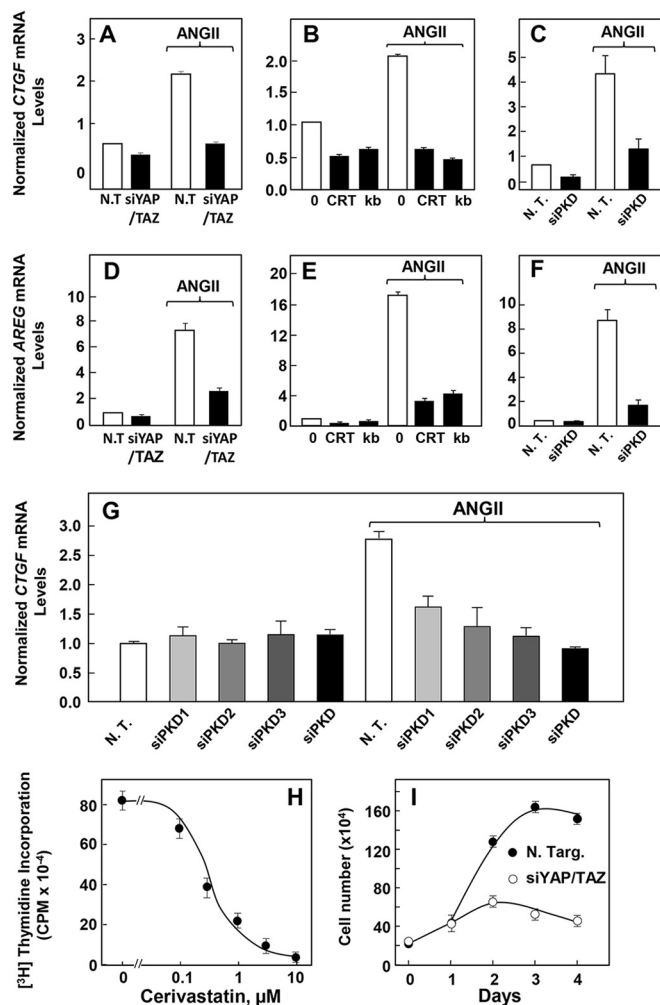
FIGURE 9. **ANG II induces increased expression of *Areg* and *Ctgf* through PKDs in IEC-18 cells.** *A* and *D,* cultures of IEC-18 cells were transfected with non-targeting siRNA (*N.T.*) or with siRNAs targeting YAP and TAZ (*siYAP/TAZ*). Then the cultures were stimulated with 10 nM ANG II for 1 h. RNA was isolated, and the relative levels (*n* = 3) of *Ctgf* (*A*) and *Areg* (*D*) mRNAs compared with *Gapdh* mRNA were measured by RT-qPCR. Similar results were obtained in two independent experiments. Data were presented as mean ± S.E. *B* and *E,* confluent cultures of IEC-18 cells were incubated in the in the absence (*0*) or presence of either 2.5 μM CRT0066101 (*CRT*) or 3.5 μM kb NB 142-70 (*kB*) for 1 h prior to stimulation of the cells without or with 10 nM ANG II for 1 h, as indicated. RNA was isolated, and the relative levels (*n* = 3) of *Ctgf* (*B*) or *Areg* (*E*) mRNA compared with *Gapdh* mRNA were measured by RT-qPCR. Data are presented as mean ± S.E. Similar results were obtained in three independent experiments. *C* and *F,* cultures of IEC-18 cells were transfected with non-targeting siRNA (*N.T.*) or with a mixture of siRNAs targeting PKD1, PKD2, and PKD3 (*siPKD*). Then the cultures were stimulated with 10 nM ANG II for 1 h. RNA was isolated, and the relative levels (*n* = 3) of *Ctgf* (*C*) or *Areg* (*F*) mRNAs compared with *Gapdh* mRNA were measured by RT-qPCR. Data are presented as mean ± S.E. Similar results were obtained in three independent experiments. *G,* cultures of IEC-18 cells were transfected with non-targeting siRNA (*N.T.*) or with either siRNAs targeting the individual PKDs, *i.e.* PKD1, PKD2, or PKD3 or a mixture of siRNAs to PKD1, PKD2, and PKD3 (*siPKD*). Then the cultures were stimulated with 10 nM ANG II for 1 h. RNA was isolated, and the relative levels (*n* = 6) of *Ctgf* mRNAs compared with *Gapdh* mRNA were measured by RT-qPCR. Data were presented as mean ± S.E. Similar results were obtained in two independent experiments. *H,* confluent cultures of IEC-18 cells were incubated in the absence or presence for 24 h with the indicated concentrations of cerivastatin in conditioned medium prior to stimulation with 10 nM ANG II for 18 h and then pulse-labeled with [³H]thymidine (0.25 μCi/ml) for 6 h. The radioactivity incorporated into acid-insoluble pools was measured in a scintillation counter. Similar results were obtained in four independent experiments. *I,* cultures of IEC-18 cells were transfected with non-targeting siRNA (*N. Targ.*) or with siRNAs targeting YAP and TAZ (*siYAP/TAZ*). Cell numbers were determined from three plates per condition each day for 4 days. Similar results were obtained in two independents experiment.

localization, phosphorylation, and transcriptional activity in intestinal epithelial cells.

As indicated above, the changes in YAP localization and phosphorylation in response to GPCR activation were transient, as YAP phosphorylation declined and translocated to the nucleus. Recent studies indicate that Rho activation and actin polymerization stimulate YAP nuclear translocation and, consequently, promote YAP/TEAD-regulated gene expression (7). In turn, PKDs can promote Rho activation and actin cytoskeleton organization in a variety of cell types (19, 62– 64). Indeed, stimulation of IEC-18 cells with ANG II for 1 h induced robust actin stress fiber formation (Fig. 10, *A* and *B*), a response prevented by either PKD inhibition with CRT0066101 (Fig. 10*A*) or siRNA-mediated knockdown of the PKDs (Fig. 10*B*). These results implying that PKDs act downstream of ANG II to induce actin remodeling in IEC-18 cells prompted us to determine whether ANG II-induced actin polymerization contributes to the second phase of YAP activation leading to YAP/TEAD-regulated genes in these cells.

We found that treatment of IEC-18 cells with Y16, a novel and potent inhibitor of Rho activation (65), abrogated actin stress fiber formation and prevented the re-entry of YAP into the nucleus (Fig. 10*C*). In line with the inhibition of YAP nuclear import, exposure to Y16 blocked the increase in *Ctgf* and *Areg* mRNA levels induced by stimulation with ANG II in IEC-18 cells (Fig. 10*D*). Exposure of IEC-18 cells to a cell-permeable C3 transferase that inactivates RhoA/B/C in intact cells also attenuated the increase in *Ctgf* and *Areg* mRNA levels in response to ANG II (data not shown). To substantiate that actin remodeling plays a role in promoting the second phase of YAP activation, we inhibited actin polymerization with latrunculin b, an agent that selectively binds G actin and blocks the formation of F-actin. Treatment of IEC-18 cells with latrunculin b inhibited YAP re-entry into the nucleus (Fig. 10*C*) and YAP/TEAD-regulated gene expression (Fig. 10*E*). Thus, inhibition of either Rho activation (Y16) or actin polymerization (latrunculin b) prevented YAP/TEAD-regulated gene expression, a hallmark of YAP nuclear entry and activation. We verified that treatment of intact IEC-18 cells with either Y16 or latrunculin b did not block PKD activation in response to ANG II stimulation (Fig. 10*F*), indicating that Rho/actin polymerization acts downstream of PKDs in ANG II-stimulated IEC-18 cells. Therefore, our results show that ANG II induces stress fiber formation via PKDs and corroborate that the PKD-dependent changes in the cytoskeleton contribute to mediate the second phase of GPCR/PKD-mediated YAP nuclear import and YAP/TEAD activation in IEC-18 cells.

Role of YAP/TEAD in GPCR/PKD-induced Mitogenic Signaling in Intestinal Epithelial Cells—In view of our results connecting PKDs with YAP regulation and given our previous results demonstrating a critical role of PKD in GPCR-mediated proliferation in intestinal epithelial cells, we next examined the biological significance of YAP in mediating the proliferative response of intestinal epithelial cells induced via GPCR/PKD activation. A recent high throughput screen of compounds capable of disrupting the nuclear localization of YAP led to the identification of statins as potent inhibitors of YAP/TAZ/TEAD transcriptional activity (66, 67). To determine the role of
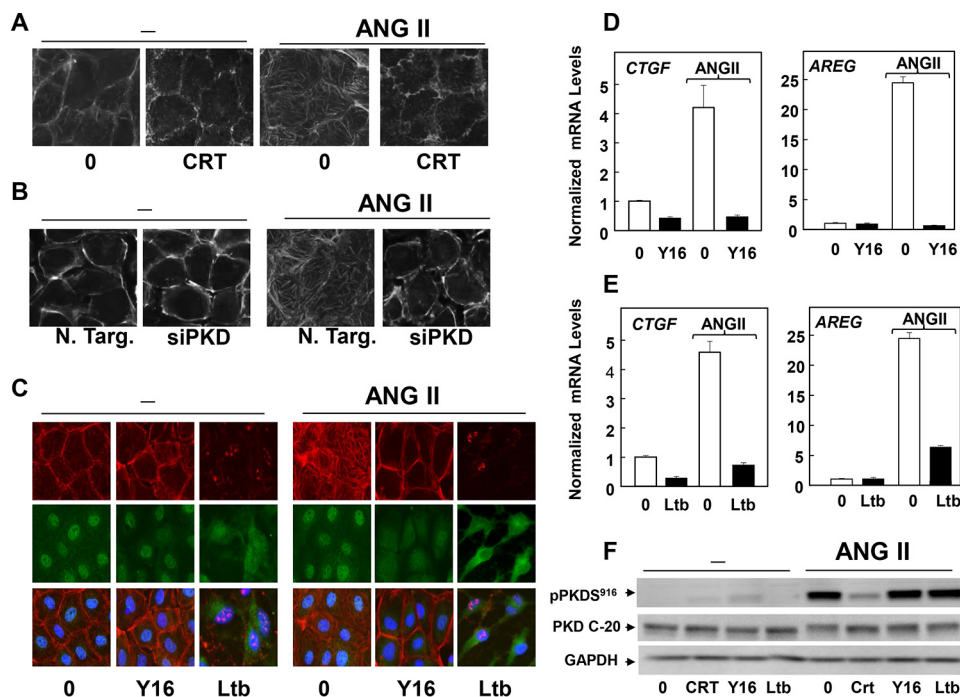
FIGURE 10. **GPCR/PKD mediates YAP re-entry into the nucleus through Rho and actin remodeling.** *A,* confluent and quiescent cultures of IEC-18 cells were incubated in the absence (*0*) or presence of 2.5 μM CRT0066101 (*CRT*) for 1 h prior to stimulation without (−) with 10 nM ANG II for 1 h. The cultures were then washed, fixed with 4% paraformaldehyde, and stained with TRITC-conjugated phalloidin. *B,* cultures of IEC-18 cells were transfected with non-targeting siRNA (*N. Targ*) or with a mixture of siRNAs targeting PKD1, PKD2, and PKD3 (*siPKD*) for 4 days. Then the cultures were stimulated with 10 nM ANG II for 1 h, washed, fixed with 4% paraformaldehyde, and stained with TRITC-conjugated phalloidin. *C,* confluent cultures of IEC-18 cells were incubated in the absence (*0*) or presence of 20 μM Y16 or 2.5 μM latrunculin B (*Ltb*) for 1 h prior to stimulation of the cells without (−) or with 10 nM ANG II for 1 h. The cultures were then washed, fixed with 4% paraformaldehyde, and stained with an antibody that detects total YAP, Hoechst 33342, to visualize the cell nuclei and TRITC-conjugated phalloidin. *D,* confluent cultures of IEC-18 cells were incubated in the absence (*0*) or presence of 20 μM Y16 for 1 h prior to stimulation of the cells without or with 10 nM ANG II for 1 h, as indicated. RNA was isolated, and the relative levels ($n = 3$) of *Ctgf* and *Areg* mRNA compared with *Gapdh* mRNA were measured by RT-qPCR. Data are presented as mean ± S.E. Similar results were obtained in three independent experiments. *E,* confluent cultures of IEC-18 cells were incubated in the absence (*0*) or presence of 2.5 μM latrunculin B for 1 h prior to stimulation of the cells without or with 10 nM ANG II for 1 h, as indicated. RNA was isolated, and the relative levels ($n = 3$) of *Ctgf* and *Areg* mRNA compared with *Gapdh* mRNA were measured by RT-qPCR. Data are presented as mean ± S.E. Similar results were obtained in three independent experiments. *F,* confluent cultures of IEC-18 cells were incubated in the absence (*0*) or presence of 2.5 μM CRT0066101 (*CRT*), 20 μM Y16, or 2.5 μM latrunculin B (*Ltb*) for 1 h prior to stimulation of the cells without (−) or with 10 nM ANG II for 1 h. Cells were then lysed with 2× SDS-PAGE sample buffer and analyzed by immunoblotting antibodies that detect PKD1 phosphorylated at Ser[916], total PKD1/2 (PKD C-20), and GAPDH. Similar results were obtained in three independent experiments.

YAP/TAZ/TEAD in GPCR-induced DNA synthesis, IEC-18 cells were treated with increasing concentrations of cerivastatin prior to stimulation with ANG II. DNA synthesis was measured by assessing [³H]thymidine incorporation into cellular nucleic acids. Cerivastatin inhibited the stimulation of DNA synthesis induced by ANG II in a dose-dependent manner (Fig. 9*H*). Other statins, including fluvastatin (3 μM) and simvastatin (10 μM), also abrogated the stimulation of DNA synthesis induced by ANG II (results not shown). Furthermore, siRNA-mediated knockdown of YAP and TAZ markedly inhibited the proliferation of IEC-18 cells (Fig. 9*I*). These results imply that the activity of YAP/TAZ is required for the proliferation of intestinal epithelial cells in response to GPCR/PKD activation.

Rapid Nuclear Exit of YAP Is Necessary for Its Function as a Transcriptional Co-activator—Subsequently, we determined whether the rapid nuclear exit of YAP is necessary for its function as a transcriptional co-activator. Using an available algorithm to predict leucine-rich nuclear export sequence (NES) that potentially mediates nuclear extrusion (68), we identified a NES in YAP within the sequence encompassed by Leu[308] to Leu[320]. Chromosome region maintenance 1 (Crm1; also referred to as exportin1) is the major receptor for the export of proteins out of the nucleus containing a leucine-rich NES.

Leptomycin B (LMB) is an antibiotic that inhibits the formation of complexes consisting of Crm1, RanGTP, and proteins containing a leucine-rich NES, thereby blocking their nuclear export (69–71). To determine whether LMB has any effect on the cellular distribution of YAP, IEC-18 cells were incubated with LMB (10 nM) for 1 h and then stimulated with ANG II for 30 min. As shown in Fig. 11, *A,* image analysis in *B,* exposure to LMB prevented the nuclear extrusion of YAP induced by ANG II. Consequently, we determined whether treatment with LMB blocks the expression of YAP/TEAD-regulated genes (*Ctgf* and *Areg*) induced by ANG II in IEC-18 cells. As shown in Fig. 11*C,* LMB markedly inhibited the increase in *Areg* and *Ctgf* mRNA levels induced by ANG II. As controls, we verified that LMB did not block YAP phosphorylation at Ser[127] and Ser[397], PKD1 autophosphorylation at Ser[916], or PKD family activation loop phosphorylation, namely phosphorylation at Ser[744] in PKD1 and equivalent residues in PKD2 and PKD3 (Fig. 11*D*). These results substantiated that LMB inhibited selectively Crm1-mediated nuclear extrusion of YAP rather than the protein kinases that act upstream of this event. The results indicate that inhibition of GPCR-induced nuclear export of YAP prevented its transcriptional co-activator activity implying that transient nuclear extrusion of YAP during the first phase is necessary for
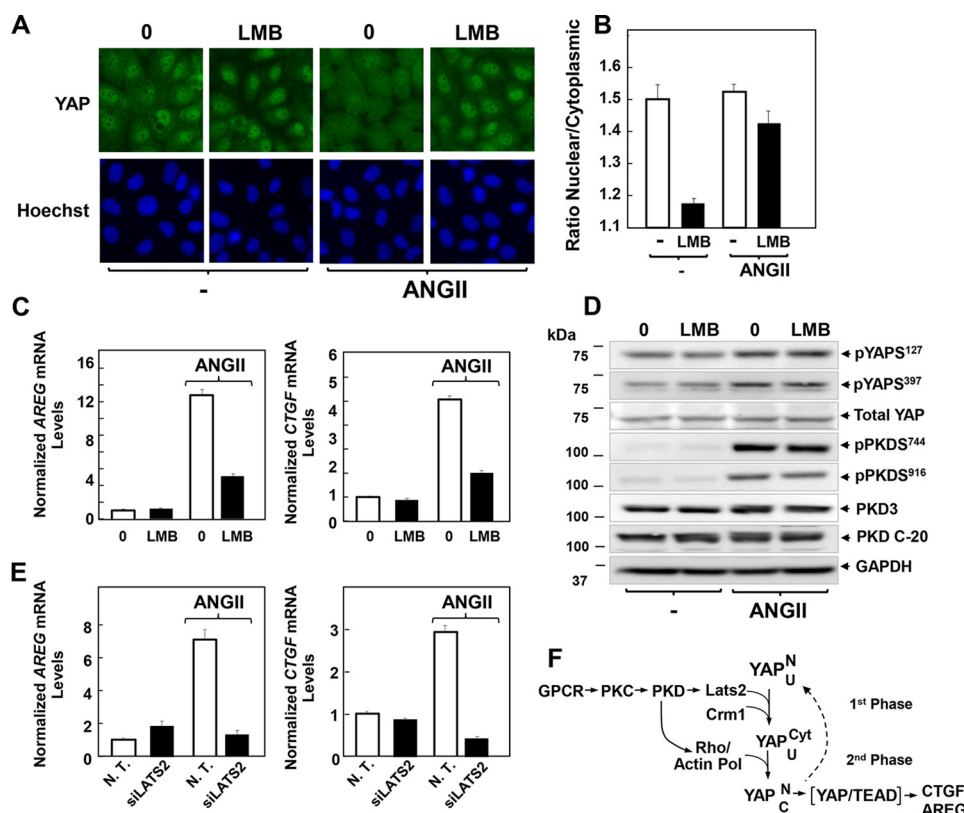
FIGURE 11. **Leptomycin B prevents the nuclear extrusion of YAP and inhibits the expression *Ctgf* and *Areg* induced by ANG II in IEC-18 cells.** *A,* confluent cultures of IEC-18 cells were incubated in the absence (*0*) or presence of 10 nM leptomycin B (*LMB*) for 1 h prior to stimulation of the cells without (−) or with 10 nM ANG II for 30 min. The cultures were then washed, fixed with 4% paraformaldehyde, and stained with an antibody that detects total YAP and with Hoechst 33342 to visualize the cell nuclei. *B,* quantification of the nuclear/cytoplasmic ratio of YAP immunofluorescence shown in *A* was determined with the CellProfiler software. The *bars* shown are the mean nuclear/cytoplasmic ratio ± S.E., $n = 5$ (~900 cells for each condition). Similar results were obtained in two independent experiments. *C,* confluent cultures of IEC-18 cells were incubated in the absence (*0*) or presence of 10 nM LMB for 1 h prior to stimulation of the cells without or with 10 nM ANG II for 1 h, as indicated. RNA was isolated, and the relative levels ($n = 3$) of *Areg* and *Ctgf* mRNA compared with *Gapdh* mRNA were measured by RT-qPCR. Data are presented as mean ± S.E. Similar results were obtained in three independent experiments. *D,* confluent cultures of IEC-18 cells were incubated in the absence (*0*) or presence of 10 nM LMB for 1 h prior to stimulation of the cells without (−) or with 10 nM ANG II for 30 min, as indicated. Cells were then lysed with 2× SDS-PAGE sample buffer and analyzed by immunoblotting with antibodies that detect YAP phosphorylated at Ser^{127} and Ser^{397}, PKD1 phosphorylated at Ser^{916}, PKDs phosphorylated at Ser^{744}, and total PKD1/2 (*PKD C-20*), PKD3, YAP, and GAPDH. Similar results were obtained in two independent experiments. *E,* cultures of IEC-18 cells were transfected with non-targeting siRNA (*N.T.*) or with siRNAs targeting Lats2 for 4 days. Then the cultures were stimulated with 10 nM ANG II for 1 h. RNA was isolated, and the relative levels ($n = 3$) of *Ctgf* and *Areg* mRNAs compared with *Gapdh* mRNA were measured by RT-qPCR. Similar results were obtained in two independent experiments. Data were presented as mean ± S.E. *F,* scheme representing a sequential model of YAP/TEAD activation in response to GPCR stimulation in intestinal epithelial cells. In non-stimulated cells, PKDs and Lats2 are in a state of very low kinase catalytic activity, although YAP is localized in the nucleus but not coupled to TEAD transcription factors, as shown by the low expression of *Ctgf* and *Areg*. GPCR stimulation induces rapid PKC/PKD activation leading to fast activation of Lats2. In turn, Lats2 mediates YAP phosphorylation at Ser^{127} which is transported out of the nucleus via Crm1 (*1st phase*). The cytoplasmic phase of YAP translocation is transitory as it re-enters the nucleus when it is dephosphorylated, and GPCR/PKD induces Rho activation and actin stress fiber formation (*Actin Pol*). YAP can now couple to TEAD thereby promoting the transcription of YAP/TEAD-regulated genes (*2nd phase*). The states of YAP are indicated in the scheme. The *superscript letters* denote localization (*N*, nuclear; *Cyt*, cytosolic), and the *subscript letters* indicate activity (*U*, uncoupled from TEAD; *C*, coupled to TEAD). Thus, we propose the following: rapid GPCR-PKC/PKD-Lats2 activation leading to Crm1-mediated YAP nuclear exit during the 1st phase followed by gradual PKD-Rho/actin polymerization leading to YAP nuclear re-entry and YAP/TEAD-regulated gene expression during the gradual 2nd phase.

its subsequent activation of TEAD-regulated genes in intestinal epithelial cells during the second phase of YAP regulation.

The results presented in Fig. 8 implied that stimulation of GPCR/PKD induces a rapid and transient YAP cytoplasmic localization in IEC-18 cells via Lats2 in IEC-18 cells, and the findings in Fig. 11 using LMB indicated that the transient nuclear extrusion of YAP is necessary for its subsequent activation of YAP/TEAD-regulated genes in these intestinal cells. Consequently, we posited that the rapid but transient GPCR-induced PKD-mediated Lats2 phosphorylation of YAP triggers YAP activation. To test this conclusion, we determined whether knockdown of Lats2 prevents the increase in the expression of YAP/TEAD-regulated genes induced by ANG II in IEC-18 cells. As shown in Fig. 11*E,*

siRNA-mediated knockdown of Lats2 prevented the increase in *Ctgf* and *Areg* mRNA levels in response to ANG II. Collectively, our results support the novel notion that GPCR-induced transient nuclear extrusion of YAP is required for its subsequent activation of TEAD-regulated genes in intestinal epithelial cells (Fig. 11*F*).

Discussion

The Hippo/YAP pathway is attracting intense interest as a key regulator of organ size, tissue regeneration, tumorigenesis, and GPCR signaling, but the mechanism(s) involved remain incompletely understood. In particular, the precise role of YAP in intestinal epithelial cell proliferation remains incompletely understood, as evidence for both growth-stimulatory and

growth-suppressive roles of YAP/TAZ has been presented (14–17).

The studies presented here revealed a novel temporal pattern of nuclear-cytoplasmic shuttling of endogenous YAP in response to GPCR activation in untransformed intestinal epithelial cells. Surprisingly, our results identified two phases in the YAP response to mitogenic GPCR agonists in these cells as follows: a rapid but transient localization of YAP to the cytoplasm followed by subsequent re-entry into the nucleus. Importantly, ANG II provoked YAP re-distribution at sub-nanomolar concentrations acting via the AT1 receptor, a GPCR that signals through $G\alpha_{q/11}$. This novel pattern of nuclear-cytoplasmic shuttling was also induced by other mitogenic stimuli, including the $G\alpha_{q/11}$-coupled receptor agonist vasopressin or serum growth factors in IEC-18 cells. A similar biphasic temporal pattern was also elicited in other intestinal epithelial cells, including rat IEC-6 and human Caco-2. These effects are clearly cell type-dependent, because mitogenic stimuli produced the opposite pattern in HEK293 or PANC-1 cells, in agreement with previous reports using these cell lines.

In other cell model systems, the subcellular distribution of YAP is controlled by its phosphorylation at Ser^{127}, a highly conserved residue phosphorylated by Lats1/2. The phosphorylation of this residue promotes the shift of YAP from the nucleus to the cytoplasm. Accordingly, we found that ANG II induced a prompt and dose-dependent increase in the phosphorylation of YAP at Ser^{127}. YAP localization and phosphorylation of Ser^{127} were tightly coupled in IEC-18 cells, as the dose responses of ANG II for eliciting YAP re-localization and phosphorylation were superimposable. In addition to Lats1/2, mammalian NDR1/2 kinases have recently been proposed to phosphorylate YAP on Ser^{127} in intestinal epithelial cells (48). However, the NDRs did not phosphorylate YAP at Ser^{397} (48), a residue targeted by Lats1/2 (49). We found that stimulation with GPCR agonists or serum induced YAP phosphorylation at Ser^{397}. Indeed, the phosphorylation of YAP at Ser^{127} and Ser^{397} was stimulated by ANG II with identical time courses and dose responses. These results suggested that ANG II induces a fast but transient YAP phosphorylation at Ser^{127} and Ser^{397} via Lats1/2 activation within intestinal epithelial IEC-18 cells. In support of this conclusion, we demonstrated that GPCR activation induced a rapid increase in Lats1/2 activity, as scored by phosphorylation at $Thr^{1079/1041}$, residues located in the hydrophobic C-terminal domain of Lats1/2 targeted by Mst1/2 and critical for Lats family activation. Importantly, knockdown of Lats2 prevented the increase in the phosphorylation of YAP at Ser^{127} and Ser^{397} and its nuclear extrusion induced by GPCR stimulation. Collectively, our results indicate that stimulation of GPCR induces rapid and transient YAP phosphorylation and cytoplasmic localization through Lats2 in IEC-18 cells.

As a first step to identify upstream pathways that mediate rapid GPCR-induced YAP nuclear-cytoplasmic shuttling and phosphorylation in intestinal epithelial cells, we tested small molecule inhibitors targeting kinases. Given the role attributed to Akt in Hippo pathway regulation in other cell types (52, 53) and the rapid Akt activation in response to ANG II in IEC-18 cells (45), we determined the effect of the Akt inhibitor GSK690693 on YAP re-localization and phosphorylation. We found that GSK690693 blocked the rapid cytoplasmic accumulation and phosphorylation at Ser^{127} and Ser^{397} of YAP induced by ANG II, but these inhibitory effects were not replicated by other Akt inhibitors, including GDC-0068 (55) and MK2206 (56). We concluded that GSK690693 potently inhibits YAP cytoplasmic localization and phosphorylation in IEC-18 cells through an Akt-independent pathway.

Although considered a selective Akt inhibitor, GSK690693 is known to inhibit PKA and novel PKCs (57). Although suppression of PKA activity within intact IEC-18 cells did not produce any detectable effect on YAP localization or phosphorylation in response to ANG II, treatment with PKC inhibitors greatly attenuated YAP cytoplasmic localization and phosphorylation at both Ser^{127} and Ser^{397}. As indicated above, the AT_1 ANG II receptor acts through $G\alpha_{q/11}$ to activate downstream signaling, including stimulation of the isoforms of the phospholipase C (PLC) family, which catalyze the hydrolysis of phosphatidylinositol 4,5-bisphosphate to produce 2-s messengers as follows: inositol 1,4,5-trisphosphate, which triggers the release of Ca^{2+} from internal stores, and diacylglycerol, which elicits cellular responses through classic (α, β, and γ) and novel (δ, ϵ, η, and θ) isoforms of PKC. In agreement with a recent report (72), the results presented here suggest that PKCs play a role in GPCR-mediated rapid regulation of YAP localization and phosphorylation, but the mechanism(s) downstream of PKC remained incompletely understood.

Our previous studies demonstrated that PKDs are rapidly activated through PKC-catalyzed phosphorylation in their kinase activation loop (29–32). Consequently, we hypothesized that YAP localization, phosphorylation, and transcriptional activity is regulated by a PKC/PKD axis in intestinal epithelial cells. Here, we presented several lines of evidence identifying a novel cross-talk between PKD and YAP. 1) Treatment with the structurally unrelated PKD inhibitors CRT0066101 and kb NB 142-70 prevented the rapid cytoplasmic accumulation induced by ANG II in IEC-18 cells. 2) The PKD inhibitors also inhibited phosphorylation of YAP at both Ser^{127} and Ser^{397} and phosphorylation of Lats1/2 at $Thr^{1079/1041}$ and $Ser^{909/872}$. 3) In dose-response studies, CRT0066101 and kb NB 142-70 prevented ANG II-induced YAP phosphorylation on Ser^{127} and rapid YAP cytoplasmic accumulation at similar concentrations. 4) Knockdown of the PKDs prevented YAP nuclear-cytoplasmic shuttling and phosphorylation at Ser^{127} and Ser^{397} in response to GPCR activation. Thus, our results demonstrate, for the first time, that the PKDs feed into the YAP pathway, as scored by YAP nuclear-cytoplasmic shuttling and phosphorylation in intestinal epithelial cells.

The changes in YAP phosphorylation and localization and Lats activation were transient, as YAP phosphorylation at Ser^{127} and Ser^{397} declined and YAP re-located to the nucleus. Furthermore, a PKD-dependent increase in actin stress fiber formation, a characteristic feature of Rho activation, contributed to mediating the second phase of GPCR/PKD-mediated YAP nuclear import in IEC-18 cells. We hypothesized that during this second phase of nuclear re-entry, YAP couples to TEAD leading to YAP/TEAD-regulated transcription. In agreement with this hypothesis, we found that stimulation of IEC-18 cells with ANG II increased the mRNA levels of the YAP/TAZ/

TEAD-regulated genes *Areg* and *Ctgf*, an effect suppressed by knockdown of YAP/TAZ. These results substantiated that ANG II induces *Areg* and *Ctgf* expression through YAP/TAZ during the second phase of GPCR-mediated YAP/TAZ regulation. Based on pharmacological and genetic approaches, we conclude that GPCR signaling stimulates YAP/TEAD transcriptional activity in intestinal epithelial cells through PKDs. Collectively, our results identify a novel role for PKDs in regulating both the rapid GPCR-induced YAP cytoplasmic localization and phosphorylation and the subsequent YAP nuclear import and transcriptional activation in intestinal epithelial cells.

Having established biphasic YAP regulation in intestinal epithelial cells via PKDs, we examined whether the second phase of YAP nuclear re-localization and activation contributes to mediate long term biological responses, including re-initiation of DNA synthesis and cell proliferation. Our recent studies with crypt-derived intestinal epithelial cells and PKD1 transgenic mice indicated that PKD1 promotes proliferation and migration of intestinal epithelial cells *in vitro* and *in vivo* (36, 38). Interestingly, PKDs and YAP were identified as components of the intestinal stem cell signature composed of 384 unique genes (73). Supporting the notion that YAP/TAZ activation contributes to mediate long term biological responses, we showed that treatment of IEC-18 cells with cerivastatin, a potent inhibitor of YAP/TAZ activity (66, 67), prevented the stimulation of DNA synthesis induced via GPCR/PKD, and knockdown of YAP/TAZ suppressed proliferation of intestinal epithelial cells.

It is generally thought that mitogenic stimuli induce rapid YAP dephosphorylation and nuclear localization, whereas growth-inhibitory signals promote YAP phosphorylation, cytoplasmic translocation, and restricted activity. Our results are of especial significance because they reveal a novel biphasic temporal pattern of nuclear-cytoplasmic shuttling and phosphorylation of YAP in response to GPCR stimulation in confluent and quiescent intestinal epithelial cells. Additional studies demonstrate, for the first time, that the PKD family controls the biphasic localization, phosphorylation, and transcriptional activity of YAP in intestinal epithelial cells. In turn, YAP is necessary for the stimulation of the proliferative response of intestinal epithelial cells to GPCR agonists that act via PKD. Interestingly, the rapid nuclear extrusion of YAP is required for the subsequent stimulation of its transcriptional co-activator activity, as shown by the results displayed in Fig. 11, obtained with LMB and knockdown of Lats2.

Taken together, our results suggest a sequential model of YAP activation in response to GPCR stimulation in intestinal epithelial cells (Fig. 11*F*). The salient features of this model are as follows. 1) In non-stimulated cells, PKDs and Lats2 are in a state of very low kinase catalytic activity, although YAP is localized in the nucleus but not coupled to TEAD transcription factors, as shown by the low expression of *Ctgf* and *Areg*. 2) GPCR stimulation induces rapid PKD activation via PKC-mediated activation loop phosphorylation. 3) Active PKDs promote fast activation of Lats2, as shown by increased phosphorylation in the hydrophobic domain and in the activation loop of this enzyme. In turn, Lats2 mediates YAP phosphorylation at Ser[127]. 4) Phosphorylated YAP is transported out of the nucleus

via an LMB-sensitive, Crm1-mediated mechanism (1st phase). 5) The cytoplasmic phase of YAP translocation is transitory as YAP re-enters into the nucleus when it is dephosphorylated at the Lats2 sites and via GPCR/PKD-induced Rho activation and actin polymerization. YAP can now couple to TEAD thereby promoting the transcription of YAP/TEAD-regulated genes (2nd phase). Thus, we envisage that the rapid but transient GPCR/PKD-induced activation of Lats2 triggers the activation of YAP that after nuclear-cytoplasmic shuttling can act as an effective co-activator of TEAD (Fig. 11*F*). Although many aspects of this sequence of events are supported by the experimental information presented here, including biochemical, genetic, and pharmacological evidence, the elucidation of the precise mechanism by which YAP is activated in the cytoplasm of intestinal epithelial cells requires further experimental work. In conclusion, the discovery of multiple points of interaction between YAP and PKD signaling identifies a novel cross-talk in epithelial signal transduction and demonstrates, for the first time, that the PKDs feed into the YAP pathway.

Experimental Procedures

Cell Culture—The non-transformed rat intestinal epithelial IEC-18 and IEC-6 cells (41, 42), originated from intestinal crypt cells, were purchased from ATCC. These cells exhibit a number of features similar to normal cells in culture, including a normal rat diploid karyotype, a strong density inhibition of growth, a lack of growth in soft agar, and resemble stem/progenitor cells (74). Cultures of IEC-18, IEC-6, and CaCo-2 cells were maintained as described previously (36, 60). Briefly, cells were cultured in Dulbecco's modified Eagle's medium (DMEM) supplemented with 10% fetal bovine serum (FBS) and penicillin/streptomycin, and kept at 37 °C in a humidified atmosphere containing 10% CO_2 and 90% air. HEK-293 cells and PANC-1 cells were maintained in culture in DMEM supplemented with 10% FBS, as described previously (51, 75). Stock cultures were sub-cultured every 3–4 days. For experimental purposes, IEC-18 cells were seeded in 35-mm dishes at a density of 2×10^5 cells/dish. Cultures were used 6 days after plating when cell density was 1.5×10^5 cells/cm^2.

Immunofluorescence—Immunofluorescence of IEC-18 cells was performed by fixing the cultures with 4% paraformaldehyde followed by permeabilization with 0.4% Triton X-100. After extensive PBS washing, fixed cells were incubated for 2 h at 25 °C in blocking buffer (BB), consisting of PBS supplemented with 5% bovine serum albumin and then stained at 4 °C overnight with a YAP (H-9) mouse mAb (1:200) diluted in BB. Subsequently, the cells were washed with PBS at 25 °C and stained at 25 °C for 60 min with AlexaFluor 488-conjugated goat anti-mouse diluted in BB (1:100) and washed again with PBS. Nuclei were stained using a Hoechst 33342 stain (1:10,000). For staining of F-actin, fixed cells were blocked with 5% bovine serum albumin in PBS. The cells were then incubated with TRITC-conjugated phalloidin (0.25 μg/ml) in PBS for 10 min at room temperature and washed five times with PBS. The samples were imaged with an epifluorescence Zeiss Axioskop and a Zeiss water objective (Achroplan 40/.75W Carl Zeiss, Inc.). Images were captured as uncompressed 24-bit TIFF files with a cooled (−12 °C) single CCD color digital camera (Pur-

suit, Diagnostic Instruments) driven by SPOT version 4.7 software. AlexaFluor 488 signals were observed with a HI Q filter set 41001 (Chroma Technology). The selected cells displayed in the appropriate figures were representative of 90% of the population.

Image Analysis—Nuclear/cytoplasmic ratios of YAP were determined using the Cell Profiler Software. The CellProfiler software was programmed as follows: sequentially, the images of Hoechst 33342 and YAP immunofluorescence at 1024 × 1024 pixel resolution were loaded. The nuclei were identified automatically using the Hoechst 33342 signal, and then the mean fluorescent intensity of YAP in each nucleus was quantified. The cytoplasmic area of measurement for YAP immunofluorescence was defined by expanding the perimeter of the nuclear outline by 10 pixels, and the mean fluorescent intensity of YAP in each cytoplasmic area was quantified. In all cases, the data were exported to Excel, and the ratio of nuclear/cytoplasmic intensity was calculated for each cell in an image field (180–200 cells/field; 6–10 fields for each experiment). The results shown are the mean ± S.E. of 6–10 fields from one experiment, a total of 1000–2000 cells as indicated in the figure legends, and each experiment was repeated at least three times.

Immunoblotting and Detection of YAP and PKD1 Phosphorylation—Serum-starved, confluent intestinal epithelial IEC-18 cells were lysed in 2× SDS-PAGE sample buffer (20 mM Tris/HCl, pH 6.8, 6% SDS, 2 mM EDTA, 4% 2-mercaptoethanol, 10% glycerol) and boiled for 10 min. After SDS-PAGE, proteins were transferred to Immobilon-P membranes. The transfer was carried out at 100 V, 0.4 A at 4 °C for 4 h using a Bio-Rad transfer apparatus. The transfer buffer consisted of 200 mM glycine, 25 mM Tris, 0.01% SDS, and 20% CH_3OH. For detection of proteins, membranes were blocked using 5% nonfat dried milk in PBS, pH 7.2, and then incubated for at least 2 h with the desired antibodies diluted in PBS containing 0.1% Tween. Primary antibodies bound to immunoreactive bands were visualized by enhanced chemiluminescence (ECL) detection with horseradish peroxidase-conjugated anti-mouse, anti-rabbit antibody and a FUJI LAS-4000 mini luminescent image analyzer.

Knockdown of PKD Family, YAP/TAZ, and Lats2 via siRNA Transfection—Silencer Select siRNA duplexes were purchased from Ambion, Life Technologies, Inc. The siRNAs were designed to target the mRNA of mouse/rat PKD1, PKD2, PKD3, YAP, and TAZ, GenBank™ mRNA sequences: Z34524.1 (PKD1), BC083592.1 (PKD2), BC092663.1 (PKD3), DQ186896.2 (YAP), BC105631.1 (TAZ), and NM_001107267.1 (Lats2). The sequences of the siRNAs were as follows; PKD1 sense, CGAUGACAAUGACAGCGAAtt, and antisense, UUCGCUGUCAUUGUCAUCGct; PKD2 sense, GUUCUAUCGUGGACCAGAAtt, and antisense, UUCUGGUCCACGAUAGAACag; PKD3 sense, GCAUUUCACAAGGCAGUAAtt, and antisense, UUACUGCCUUGUGAAAUGCtg; YAP sense, GUUUACUACAUAAACCAUAtt, and antisense UAUGGUUUAUGUAGUAAACtt; TAZ sense, GGAUGGACUUCAUUUUGGAtt, and antisense, UCCAAAAUGAAGUCCAUCCct; and Lats2 sense, CCUACGCAGGUGAAACUCAtt, and antisense, UGAGUUUCACCUGCGUAGGga. For siRNA transfection, the reverse transfection method was used. The siRNA

pool was mixed with Lipofectamine RNAiMAX (Invitrogen) according to the manufacturer's protocol and added to 35-mm dishes. IEC-18 cells were then plated on top of the siRNA/Lipofectamine RNAiMAX complex at a density of 2 × 10^5 cells/35-mm dish in DMEM containing 10% FBS. Control transfections were carried out with Silencer Select Negative Control No. 1 (catalog no. 4390844, (Invitrogen). Three to 4 days after transfection, cells were used for experiments and subsequent Western blotting analysis.

Immunoprecipitation of YAP—Confluent IEC-18 cells were lysed in buffer containing 20 mM Tris/HCl, pH 7.5, 1% Triton X-100, 150 mM NaCl, 1 mM Na_2EDTA, 1 mM EGTA, 2.5 mM sodium pyrophosphate, 1 mM β-glycerophosphate, 1 mM Na_3VO_4, 1 μg/ml leupeptin and 1 mM 4-(2-aminoethyl)-benzenesulfonyl fluoride, hydrochloride (Pefabloc). YAP was immunoprecipitated from the cell extracts with a YAP (H-9) antibody from Santa Cruz Biotechnology. The immune complexes were recovered using protein-G coupled to agarose.

Quantitative Reverse Transcription PCR (qRT-PCR)—Relative transcript expression levels of *Areg* and *Ctgf* were determined by qRT-PCR using a SYBR Green-based method. Briefly, total RNA was extracted from cells by using TRIzol reagent (Ambion, Life Technologies, Inc.). Reverse transcription was performed with the iScript reverse transcription supermix (Bio-Rad), using 1 μg of total input RNA. The synthesized cDNA samples were used as templates for the real time (RT) PCR analysis. All reactions were performed using the LightCycler480 system (Roche Applied Science), and the amplifications were done using the SsoAdvanced™ Universal SYBR® Green Supermix (Bio-Rad). Gene-specific rat oligonucleotide primers for *Areg* (Unique Assay ID, qRnoCID0001606), *Ctgf* (Unique Assay ID, qRnoCED0001593), and *Gapdh* (Unique Assay ID, qRnoCID0057018) were purchased from Bio-Rad.

[^{3}H]Thymidine Incorporation into DNA—IEC-18 cells were plated and grown in 3.5-cm tissue culture plates for 5 days in DMEM with 2 mM glutamine, 1 mM sodium pyruvate, and 10% FBS. To start the experiment, the specified concentration of inhibitor was added to the conditioned medium (4–6 cultures used for each condition). After 18 h of incubation, the cultures were pulse-labeled for 6 h with [^{3}H]thymidine (0.25 Ci/ml), fixed with 5% trichloroacetic acid, and washed twice with ethanol. Acid-insoluble pools corresponding to DNA were solubilized in 0.1 N NaOH with 1% SDS and counted in a liquid scintillation counter.

Materials—DMEM, FBS, goat anti-mouse IgG secondary antibody conjugated to Alexa Fluor 488 and Silencer Select siRNAs were obtained from Invitrogen. Angiotensin II (ANG II), vasopressin, LMB, losartan, latrunculin b, and phalloidin-TRITC were obtained from Sigma. The kinase inhibitors kb NB 142-70, CRT0066101, H89, GSK690693, Gö6983, and GF 109203X were from R&D Systems (Minneapolis, MN), and MK-2206 and GDC-0068 were from Selleckchem (Boston). The Rho inhibitor II, Y16, was purchased from EMD Millipore (Billerica, MA). Primary antibodies used were as follows: YAP (H-9, sc-271134; final dilution 1:200 for immunofluorescence, 1:400 for Western blotting, and 1:100 for immunoprecipitation); PKD C-20 (sc-639; final dilution 1:400 for Western blotting) and GAPDH (sc-365062; final dilution 1:400) (Santa Cruz

Biotechnology); phospho-YAP Ser[127] (D9W2I, 13008; final dilution 1:1000), phospho-YAP Ser[397] (D1E7Y, 13619; final dilution 1:1000), PKD3 (5655; final dilution 1:1000), phospho-Lats1 Ser[909] (9157; final dilution 1:1000), and phospho-Lats1 Thr[1079] (D57D3, 8654; final dilution 1:1000) (all from Cell Signaling Technology Danvers, MA)). The equivalent residues in Lats2 are Ser[872] and Thr[1041], respectively. Total Lats2 was detected with an antibody from Novus Biologicals (NB200-199; final dilution 1:1000). RT-qPCR reagents were purchased from Bio-Rad. All other reagents were of the highest grade available

References

1. Crosnier, C., Stamataki, D., and Lewis, J. (2006) Organizing cell renewal in the intestine: stem cells, signals and combinatorial control. *Nat. Rev. Genet.* **7,** 349–359

2. Rozengurt, E., and Walsh, J. H. (2001) Gastrin, CCK, signaling, and cancer. *Annu. Rev. Physiol.* **63,** 49–76

3. Rozengurt, E. (2007) Mitogenic signaling pathways induced by G protein-coupled receptors. *J. Cell Physiol.* **213,** 589–602

4. Raufman, J.-P., Samimi, R., Shah, N., Khurana, S., Shant, J., Drachenberg, C., Xie, G., Wess, J., and Cheng, K. (2008) Genetic ablation of M3 muscarinic receptors attenuates murine colon epithelial cell proliferation and neoplasia. *Cancer Res.* **68,** 3573–3578

5. Rey, O., Chang, W., Bikle, D., Rozengurt, N., Young, S. H., and Rozengurt, E. (2012) Negative cross-talk between calcium-sensing receptor and β-catenin signaling systems in colonic epithelium. *J. Biol. Chem.* **287,** 1158–1167

6. Lee, S. J., Leoni, G., Neumann, P. A., Chun, J., Nusrat, A., and Yun, C. C. (2013) Distinct phospholipase C-β isozymes mediate lysophosphatidic acid receptor 1 effects on intestinal epithelial homeostasis and wound closure. *Mol. Cell. Biol.* **33,** 2016–2028

7. Yu, F.-X., and Guan, K.-L. (2013) The Hippo pathway: regulators and regulations. *Genes. Dev.* **27,** 355–371

8. Avruch, J., Zhou, D., Fitamant, J., Bardeesy, N., Mou, F., and Barrufet, L. R. (2012) Protein kinases of the Hippo pathway: regulation and substrates. *Semin. Cell Dev. Biol.* **23,** 770–784

9. Zheng, Y., Wang, W., Liu, B., Deng, H., Uster, E., and Pan, D. (2015) Identification of happyhour/MAP4K as Alternative Hpo/Mst-like Kinases in the hippo kinase cascade. *Dev. Cell* **34,** 642–655

10. Meng, Z., Moroishi, T., Mottier-Pavie, V., Plouffe, S. W., Hansen, C. G., Hong, A. W., Park, H. W., Mo, J.-S., Lu, W., Lu, S., Flores, F., Yu, F.-X., Halder, G., and Guan, K.-L. (2015) MAP4K family kinases act in parallel to MST1/2 to activate LATS1/2 in the Hippo pathway. *Nat. Commun.* **6,** 8357

11. Moroishi, T., Hansen, C. G., and Guan, K.-L. (2015) The emerging roles of YAP and TAZ in cancer. *Nat. Rev. Cancer* **15,** 73–79

12. Chen, C.-L., Tsukamoto, H., Liu, J.-C., Kashiwabara, C., Feldman, D., Sher, L., Dooley, S., French, S. W., Mishra, L., Petrovic, L., Jeong, J. H., and Machida, K. (2013) Reciprocal regulation by TLR4 and TGF-β in tumor-initiating stem-like cells. *J. Clin. Invest.* **123,** 2832–2849

13. Shanzer, M., Ricardo-Lax, I., Keshet, R., Reuven, N., and Shaul, Y. (2015) The polyomavirus middle T-antigen oncogene activates the Hippo pathway tumor suppressor Lats in a Src-dependent manner. *Oncogene* **34,** 4190–4198

14. Barry, E. R., Morikawa, T., Butler, B. L., Shrestha, K., de la Rosa, R., Yan, K. S., Fuchs, C. S., Magness, S. T., Smits, R., Ogino, S., Kuo, C. J., and

15. Camargo, F. D. (2013) Restriction of intestinal stem cell expansion and the regenerative response by YAP. *Nature* **493,** 106–110

15. Lee, K.-W., Lee, S. S., Kim, S.-B., Sohn, B. H., Lee, H.-S., Jang, H.-J., Park, Y.-Y., Kopetz, S., Kim, S. S., Oh, S. C., and Lee, J.-S. (2015) Significant association of oncogene YAP1 with poor prognosis and cetuximab resistance in colorectal cancer patients. *Clin. Cancer Res.* **21,** 357–364

16. Imajo, M., Ebisuya, M., and Nishida, E. (2015) Dual role of YAP and TAZ in renewal of the intestinal epithelium. *Nat Cell Biol.* **17,** 7–19

17. Hong, A. W., Meng, Z., and Guan, K.-L. (2016) The Hippo pathway in intestinal regeneration and disease. *Nat. Rev. Gastroenterol. Hepatol.* **13,** 324–337

18. Rozengurt, E., Rey, O., and Waldron, R. T. (2005) Protein kinase D signaling. *J. Biol. Chem.* **280,** 13205–13208

19. Rozengurt, E. (2011) Protein kinase D signaling: multiple biological functions in health and disease. *Physiology* **26,** 23–33

20. Yuan, J., Slice, L., Walsh, J. H., and Rozengurt, E. (2000) Activation of protein kinase D by signaling through the α subunit of the heterotrimeric G protein G$_q$. *J. Biol. Chem.* **275,** 2157–2164

21. Yuan, J., Slice, L. W., and Rozengurt, E. (2001) Activation of protein kinase D by signaling through Rho and the α subunit of the heterotrimeric G protein G13. *J. Biol. Chem.* **276,** 38619–38627

22. Paolucci, L., Sinnett-Smith, J., and Rozengurt, E. (2000) Lysophosphatidic acid rapidly induces protein kinase D activation through a pertussis toxin-sensitive pathway. *Am. J. Physiol. Cell Physiol.* **278,** C33–C39

23. Chiu, T., and Rozengurt, E. (2001) PKD in intestinal epithelial cells: rapid activation by phorbol esters, LPA, and angiotensin through PKC. *Am. J. Physiol. Cell Physiol.* **280,** C929–C942

24. Yuan, J., Slice, L. W., Gu, J., and Rozengurt, E. (2003) Cooperation of Gq, Gi, and G12/13 in protein kinase D activation and phosphorylation induced by lysophosphatidic acid. *J. Biol. Chem.* **278,** 4882–4891

25. Yuan, J., Rey, O., and Rozengurt, E. (2006) Activation of protein kinase D3 by signaling through Rac and the α subunits of the heterotrimeric G proteins G12 and G13. *Cell. Signal.* **18,** 1051–1062

26. Waldron, R. T., Innamorati, G., Torres-Marquez, M. E., Sinnett-Smith, J., and Rozengurt, E. (2012) Differential PKC-dependent and -independent PKD activation by G protein α subunits of the Gq family: selective stimulation of PKD Ser[748] autophosphorylation by Gαq. *Cell. Signal.* **24,** 914–921

27. Valverde, A. M., Sinnett-Smith, J., Van Lint, J., and Rozengurt, E. (1994) Molecular cloning and characterization of protein kinase D: a target for diacylglycerol and phorbol esters with a distinctive catalytic domain. *Proc. Natl. Acad. Sci. U.S.A.* **91,** 8572–8576

28. Johannes, F. J., Prestle, J., Eis, S., Oberhagemann, P., and Pfizenmaier, K. (1994) PKCu is a novel, atypical member of the protein kinase C family. *J. Biol. Chem.* **269,** 6140–6148

29. Iglesias, T., Waldron, R. T., and Rozengurt, E. (1998) Identification of *in vivo* phosphorylation sites required for protein kinase D activation. *J. Biol. Chem.* **273,** 27662–27667

30. Waldron, R. T., Rey, O., Iglesias, T., Tugal, T., Cantrell, D., and Rozengurt, E. (2001) Activation loop Ser[744] and Ser[748] in protein kinase D are transphosphorylated *in vivo*. *J. Biol. Chem.* **276,** 32606–32615

31. Waldron, R. T., and Rozengurt, E. (2003) Protein kinase C phosphorylates protein kinase D activation loop Ser[744] and Ser[748] and releases autoinhibition by the pleckstrin homology domain. *J. Biol. Chem.* **278,** 154–163

32. Rey, O., Reeve, J. R., Jr., Zhukova, E., Sinnett-Smith, J., and Rozengurt, E. (2004) G protein-coupled receptor-mediated phosphorylation of the activation loop of protein kinase D: dependence on plasma membrane translocation and protein kinase Cε. *J. Biol. Chem.* **279,** 34361–34372

33. Matthews, S. A., Rozengurt, E., and Cantrell, D. (1999) Characterization of serine 916 as an *in vivo* autophosphorylation site for protein kinase D/protein kinase Cμ. *J. Biol. Chem.* **274,** 26543–26549

34. Sinnett-Smith, J., Zhukova, E., Hsieh, N., Jiang, X., and Rozengurt, E. (2004) Protein kinase D potentiates DNA synthesis induced by Gq-coupled receptors by increasing the duration of ERK signaling in Swiss 3T3 cells. *J. Biol. Chem.* **279,** 16883–16893

35. Sinnett-Smith, J., Jacamo, R., Kui, R., Wang, Y. M., Young, S. H., Rey, O., Waldron, R. T., and Rozengurt, E. (2009) Protein kinase D mediates mitogenic signaling by Gq-coupled receptors through protein kinase C-inde-

pendent regulation of activation Loop Ser[744] and Ser[748] phosphorylation. *J. Biol. Chem.* **284,** 13434–13445

36. Sinnett-Smith, J., Rozengurt, N., Kui, R., Huang, C., and Rozengurt, E. (2011) Protein kinase D1 mediates stimulation of DNA synthesis and proliferation in intestinal epithelial IEC-18 cells and in mouse intestinal crypts. *J. Biol. Chem.* **286,** 511–520

37. Jacamo, R., Sinnett-Smith, J., Rey, O., Waldron, R. T., and Rozengurt, E. (2008) Sequential protein kinase C (PKC)-dependent and PKC-independent protein kinase D catalytic activation via Gq-coupled receptors: differential regulation of activation loop Ser(744) and Ser(748) phosphorylation. *J. Biol. Chem.* **283,** 12877–12887

38. Young, S. H., Rozengurt, N., Sinnett-Smith, J., and Rozengurt, E. (2012) Rapid protein kinase D1 signaling promotes migration of intestinal epithelial cells. *Am. J. Physiol. Gastrointest. Liver Physiol.* **303,** G356–366

39. Chiu, T., Wu, S. S., Santiskulvong, C., Tangkijvanich, P., Yee, H. F., Jr., and Rozengurt, E. (2002) Vasopressin-mediated mitogenic signaling in intestinal epithelial cells. *Am. J. Physiol. Cell Physiol.* **282,** C434–C450

40. Rey, O., Zhukova, E., Sinnett-Smith, J., and Rozengurt, E. (2003) Vasopressin-induced intracellular redistribution of protein kinase D in intestinal epithelial cells. *J. Cell Physiol.* **196,** 483–492

41. Quaroni, A., Wands, J., Trelstad, R. L., and Isselbacher, K. J. (1979) Epithelioid cell cultures from rat small intestine. Characterization by morphologic and immunologic criteria. *J. Cell Biol.* **80,** 248–265

42. Quaroni, A., and May, R. J. (1980) Establishment and characterization of intestinal epithelial cell cultures. *Methods Cell Biol.* **21B,** 403–427

43. Wu, S. S., Chiu, T., and Rozengurt, E. (2002) ANG II and LPA induce Pyk2 tyrosine phosphorylation in intestinal epithelial cells: role of Ca^{2+}, PKC, and Rho kinase. *Am. J. Physiol. Cell Physiol.* **282,** C1432–C1444

44. Chiu, T., Santiskulvong, C., and Rozengurt, E. (2003) ANG II stimulates PKC-dependent ERK activation, DNA synthesis, and cell division in intestinal epithelial cells. *Am. J. Physiol. Gastrointest. Liver Physiol.* **285,** G1–G11

45. Chiu, T., Santiskulvong, C., and Rozengurt, E. (2005) EGF receptor transactivation mediates ANG II-stimulated mitogenesis in intestinal epithelial cells through the PI3-kinase/Akt/mTOR/p70S6K1 signaling pathway. *Am. J. Physiol. Gastrointest. Liver Physiol.* **288,** G182–G194

46. Young, S. H., and Rozengurt, E. (2006) Qdot nanocrystal conjugates conjugated to bombesin or ANG II label the cognate G protein-coupled receptor in living cells. *Am. J. Physiol. Cell Physiol.* **290,** C728–C732

47. Slice, L. W., Chiu, T., and Rozengurt, E. (2005) Angiotensin II and epidermal growth factor induce cyclooxygenase-2 expression in intestinal epithelial cells through small GTPases using distinct signaling pathways. *J. Biol. Chem.* **280,** 1582–1593

48. Zhang, L., Tang, F., Terracciano, L., Hynx, D., Kohler, R., Bichet, S., Hess, D., Cron, P., Hemmings, B. A., Hergovich, A., and Schmitz-Rohmer, D. (2015) NDR Functions as a physiological YAP1 kinase in the intestinal epithelium. *Curr. Biol.* **25,** 296–305

49. GC0068Zhao, B., Li, L., Tumaneng, K., Wang, C.-Y., and Guan, K.-L. (2010) A coordinated phosphorylation by Lats and CK1 regulates YAP stability through SCFβ-TRCP. *Genes Dev.* **24,** 72–85

50. Guha, S., Rey, O., and Rozengurt, E. (2002) Neurotensin induces protein kinase C-dependent protein kinase D activation and DNA synthesis in human pancreatic carcinoma cell line PANC-1. *Cancer Res.* **62,** 1632–1640

51. Soares, H. P., Ni, Y., Kisfalvi, K., Sinnett-Smith, J., and Rozengurt, E. (2013) Different patterns of Akt and ERK feedback activation in response to rapamycin, active-site mTOR inhibitors and metformin in pancreatic cancer cells. *PLoS ONE* **8,** e57289

52. Kim, D., Shu, S., Coppola, M. D., Kaneko, S., Yuan, Z.-Q., and Cheng, J. Q. (2010) Regulation of proapoptotic mammalian ste20-like kinase MST2 by the IGF1-Akt pathway. *PLoS ONE* **5,** e9616

53. Collak, F. K., Yagiz, K., Luthringer, D. J., Erkaya, B., and Cinar, B. (2012) Threonine-120 phosphorylation regulated by phosphoinositide-3-kinase/Akt and mammalian target of rapamycin pathway signaling limits the antitumor activity of mammalian sterile 20-Like kinase 1. *J. Biol. Chem.* **287,** 23698–23709

54. Rhodes, N., Heerding, D. A., Duckett, D. R., Eberwein, D. J., Knick, V. B., Lansing, T. J., McConnell, R. T., Gilmer, T. M., Zhang, S.-Y., Robell, K.,

Kahana, J. A., Geske, R. S., Kleymenova, E. V., Choudhry, A. E., Lai, Z., *et al.* (2008) Characterization of an Akt kinase inhibitor with potent pharmacodynamic and antitumor activity. *Cancer Res.* **68,** 2366–2374

55. Blake, J. F., Xu, R., Bencsik, J. R., Xiao, D., Kallan, N. C., Schlachter, S., Mitchell, I. S., Spencer, K. L., Banka, A. L., Wallace, E. M., Gloor, S. L., Martinson, M., Woessner, R. D., Vigers, G. P., Brandhuber, B. J., *et al.* (2012) Discovery and preclinical pharmacology of a selective ATP-competitive Akt inhibitor (GDC-0068) for the treatment of human tumors. *J. Med. Chem.* **55,** 8110–8127

56. Hirai, H., Sootome, H., Nakatsuru, Y., Miyama, K., Taguchi, S., Tsujioka, K., Ueno, Y., Hatch, H., Majumder, P. K., Pan, B.-S., and Kotani, H. (2010) MK-2206, an allosteric Akt inhibitor, enhances antitumor efficacy by standard chemotherapeutic agents or molecular targeted drugs *in vitro* and *in vivo*. *Mol. Cancer Ther.* **9,** 1956–1967

57. Davis, M. I., Hunt, J. P., Herrgard, S., Ciceri, P., Wodicka, L. M., Pallares, G., Hocker, M., Treiber, D. K., and Zarrinkar, P. P. (2011) Comprehensive analysis of kinase inhibitor selectivity. *Nat. Biotechnol.* **29,** 1046–1051

58. Harikumar, K. B., Kunnumakkara, A. B., Ochi, N., Tong, Z., Deorukhkar, A., Sung, B., Kelland, L., Jamieson, S., Sutherland, R., Raynham, T., Charles, M., Bagherzadeh, A., Bagherazadeh, A., Foxton, C., Boakes, A., Farooq, M., Maru, D., Diagaradjane, P., Matsuo, Y., Sinnett-Smith, J., Gelovani, J., Krishnan, S., Aggarwal, B. B., Rozengurt, E., Ireson, C. R., and Guha, S. (2010) A novel small-molecule inhibitor of protein kinase D blocks pancreatic cancer growth *in vitro* and *in vivo*. *Mol. Cancer Ther.* **9,** 1136–1146

59. Sinnett-Smith, J., Ni, Y., Wang, J., Ming, M., Young, S. H., and Rozengurt, E. (2014) Protein kinase D1 mediates class IIa histone deacetylase phosphorylation and nuclear extrusion in intestinal epithelial cells: role in mitogenic signaling. *Am. J. Physiol. Cell Physiol.* **306,** C961–C971

60. Ni, Y., Sinnett-Smith, J., Young, S. H., and Rozengurt, E. (2013) PKD1 mediates negative feedback of PI3K/Akt activation in response to G protein-coupled receptors. *PLoS ONE* **8,** e73149

61. Moroishi, T., Park, H. W., Qin, B., Chen, Q., Meng, Z., Plouffe, S. W., Taniguchi, K., Yu, F.-X., Karin, M., Pan, D., and Guan, K.-L. (2015) A YAP/TAZ-induced feedback mechanism regulates Hippo pathway homeostasis. *Genes Dev.* **29,** 1271–1284

62. Eiseler, T., Döppler, H., Yan, I. K., Kitatani, K., Mizuno, K., and Storz, P. (2009) Protein kinase D1 regulates cofilin-mediated F-actin reorganization and cell motility through slingshot. *Nat. Cell Biol.* **11,** 545–556

63. Scholz, R.-P., Gustafsson, J. O. R., Hoffmann, P., Jaiswal, M., Ahmadian, M. R., Eisler, S. A., Erlmann, P., Schmid, S., Hausser, A., and Olayioye, M. A. (2011) The tumor suppressor protein DLC1 is regulated by PKD-mediated GAP domain phosphorylation. *Exp. Cell Res.* **317,** 496–503

64. Pusapati, G. V., Eiseler, T., Rykx, A., Vandoninck, S., Derua, R., Waelkens, E., Van Lint, J., von Wichert, G., and Seufferlein, T. (2012) Protein kinase D regulates RhoA activity via rhotekin phosphorylation. *J. Biol. Chem.* **287,** 9473–9483

65. Shang, X., Marchioni, F., Evelyn, C. R., Sipes, N., Zhou, X., Seibel, W., Wortman, M., and Zheng, Y. (2013) Small-molecule inhibitors targeting G-protein-coupled Rho guanine nucleotide exchange factors. *Proc. Natl. Acad. Sci. U.S.A.* **110,** 3155–3160

66. Sorrentino, G., Ruggeri, N., Specchia, V., Cordenonsi, M., Mano, M., Dupont, S., Manfrin, A., Ingallina, E., Sommaggio, R., Piazza, S., Rosato, A., Piccolo, S., and Del Sal, G. (2014) Metabolic control of YAP and TAZ by the mevalonate pathway. *Nat. Cell Biol.* **16,** 357–366

67. Wang, Z., Wu, Y., Wang, H., Zhang, Y., Mei, L., Fang, X., Zhang, X., Zhang, F., Chen, H., Liu, Y., Jiang, Y., Sun, S., Zheng, Y., Li, N., and Huang, L. (2014) Interplay of mevalonate and Hippo pathways regulates RHAMM transcription via YAP to modulate breast cancer cell motility. *Proc. Natl. Acad. Sci. U.S.A.* **111,** E89–E98

68. la Cour, T., Kiemer, L., Mølgaard, A., Gupta, R., Skriver, K., and Brunak, S. (2004) Analysis and prediction of leucine-rich nuclear export signals. *Protein Eng. Des. Sel.* **17,** 527–536

69. Fornerod, M., Ohno, M., Yoshida, M., and Mattaj, I. W. (1997) CRM1 is an export receptor for leucine-rich nuclear export signals. *Cell* **90,** 1051–1060

70. Ossareh-Nazari, B., Bachelerie, F., and Dargemont, C. (1997) Evidence for

a role of CRM1 in signal-mediated nuclear protein export. *Science* **278,** 141–144

71. Wolff, B., Sanglier, J.-J., and Wang, Y. (1997) Leptomycin B is an inhibitor of nuclear export: inhibition of nucleo-cytoplasmic translocation of the human immunodeficiency virus type 1 (HIV-1) Rev protein and Rev-dependent mRNA. *Chem. Biol.* **4,** 139–147

72. Gong, R., Hong, A. W., Plouffe, S. W., Zhao, B., Liu, G., Yu, F.-X., Xu, Y., and Guan, K.-L. (2015) Opposing roles of conventional and novel PKC isoforms in Hippo-YAP pathway regulation. *Cell Res.* **25,** 985–988

73. Muñoz, J., Stange, D. E., Schepers, A. G., van de Wetering, M., Koo, B.-K.,

Itzkovitz, S., Volckmann, R., Kung, K. S., Koster, J., Radulescu, S., Myant, K., Versteeg, R., Sansom, O. J., van Es, J. H., Barker, N., van Oudenaarden, A., Mohammed, S., Heck, A. J., and Clevers, H. (2012) The Lgr5 intestinal stem cell signature: robust expression of proposed quiescent +4 cell markers. *EMBO J.* **31,** 3079–3091

74. Suh, E., and Traber, P. G. (1996) An intestine-specific homeobox gene regulates proliferation and differentiation. *Mol. Cell. Biol.* **16,** 619–625

75. Young, S. H., and Rozengurt, E. (2002) Amino acids and Ca^{2+} stimulate different patterns of Ca^{2+} oscillations through the Ca^{2+}-sensing receptor. *Am. J. Physiol. Cell Physiol.* **282,** C1414–C1422